Study on the role of protein arginine methyltransferase 1 (PRMT1) in the development of the central nervous system

中枢神経系発達過程における アルギニンメチル化酵素 PRMT1 の機能解析

2016

筑波大学グローバル教育院

School of the Integrative and Global Majors in

University of Tsukuba

Ph.D. Program in Human Biology

Misuzu Hashimoto

Contents

Study on the role of protein arginine methyltransferase 1 (PRMT1) in the development of the central nervous system

Chapter I.

Preface

The central nervous system (CNS) is one of the most complex organs in our body. However, its precise mechanism underlying appropriate development and functional homeostasis were not largely understood. One reason for the complexity is because CNS parenchyma is composed of three cell types including neurons, astrocytes, and oligodendrocytes, and all of them are originally derived from neural stem cells (NSCs) (Fig. I-1). Additionally, different subtypes neuron that are unique to each brain region are essential for sophisticated functions including cognition, emotion, thinking, learning, and social interaction (1, 2). As neuronal connectivity and its activity had been thought to be the principal mechanism for these roles, neurons were extensively studied in neuroscience field. Meanwhile, the importance of glial cells including astrocytes and oligodendrocytes had been overlooked as they were considered to be supportive cells and less important compared with neurons. However, growing number of studies demonstrated that activity of glia are also essential for homeostasis of the CNS tissues (3). Astrocyte is the most abundant glial cells in the CNS and it structurally supports neuron also by making a contact with neuronal synapses. In addition, astrocytes have various roles including blood-brain barrier formation, activation in response to brain

injury, and supporting other glia (4, 5, 6). Oligodendrocyte wraps around axons and forms a structure called myelin which serves as insulator for rapid saltatory conduction. It is also known to metabolically support axons (7, 8). Recently it has been reported that oligodendrocyte itself is activated in response to axonal signal (9). In sum, to understand the complexity of the CNS, it is necessary to understand the developmental regulation and the network of both neuron and glia.

For the CNS development, NSCs have to proliferate and must be specified to progenitor cells of neuron or glia at appropriate timings and all of cells have to migrate to proper region of the CNS (10). The mechanism of these processes is not totally understood yet, however, importance of cell-type specific transcription factors, microRNA (miRNA), ligands, and chromatin remodeling factors has been emphasized in a number of neurodevelopmental studies (11, 12) (Fig. I-1).

Post-translational modification of proteins is now widely known to be essential for protein structure and function. The major modifications include methylation, acetylation, phosphorylation, and ubiquitination. Among these, protein arginine methylation has been proven to be important for a wide variety of cellular mechanisms mainly by *in vitro* studies. Protein arginine methylation is catalyzed by a family of arginine methyltransferases. So far 11 members (PRMT1-11) have been identified in mammals and they have different cellular localization and substrate specificity. Although PRMT10 and 11 are not well characterized yet, PRMT1-9 are classified into two types depending on the modes of substrate methylation (13, 14) (Fig. I-2). Type I PRMTs including PRMT1, 2, 3, 4, 6, and 8 catalyzes the formation of

monomethyl arginine (MMA) by adding the first methyl group to ω-guanidino nitrogen and also forms asymmetric dimethyl arginine (ADMA) by adding the second methyl group to the same ω-guanidino nitrogen. On the other hand, type II PRMTs such as PRMT5, 7, and 9 produce MMA and symmetric dimethyl arginine (SDMA). Among these, PRMT1 was most extensively studied because it has been shown to be a major type I PRMT in mammalian cells and tissues (15). Growing number of studies have reported new substrates of PRMT1 and now it is widely accepted that PRMT1 is involved in various cellular processes such as cell survival, transcriptional control, and signal transduction by methylating histone and none-histone proteins (16-20). However, its *in vivo* function was poorly understood due to lack of appropriate genetic models.

Recent studies have demonstrated that post-translational modifications regulate CNS development by controlling the timing of gene expression which is important for cell specification and differentiation. Whereas PRMT1 is ubiquitously expressed in the adult mouse tissues (21-24), it has been shown to have the highest expression in the CNS during the early stage of mouse embryo, implicating its regulatory role for the organ formation. As described above, as NSCs is the common origin of neuron and glia, I aimed to investigate the physiological role of PRMT1 in NSCs at *in vivo* level. In the present study, I looked into the role of protein arginine methyltransferase by generating CNS-specific gene knockout mice and unexpectedly found its critical role in oligodendroglial development. This study provides *in vivo* evidence that arginine methyltransferase is indispensable for proper CNS development by controlling oligodendroglial lineage progression.

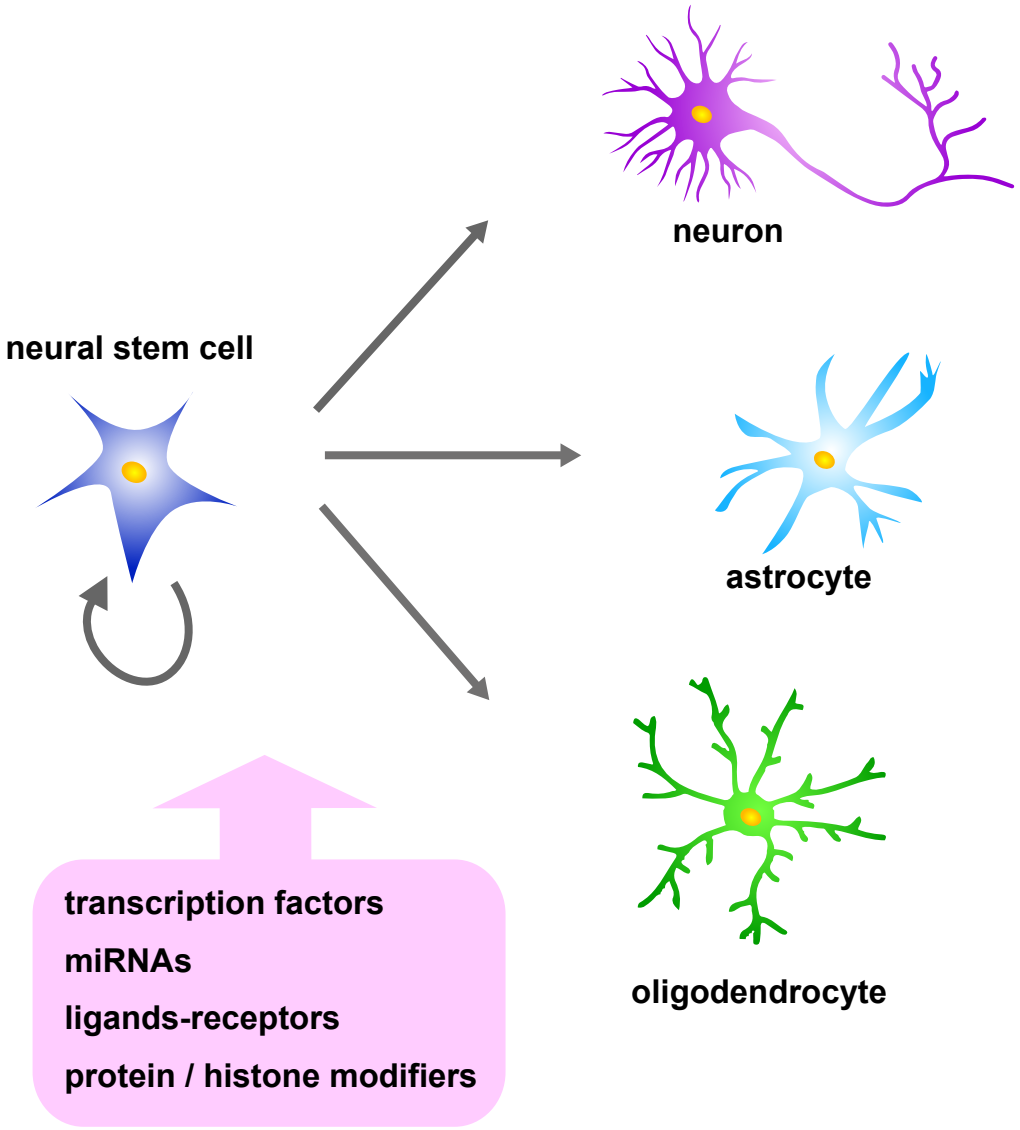

Fig. I-1. Development of the central nervous tissues

In mammals, CNS parenchyma is composed of neuron, astrocyte, and oligodendrocyte. The three cell types are originally differentiated from neural stem cells at various levels of regulation such as transcription factors, microRNAs, ligand-receptors, and factors that alters protein or histone modifications.

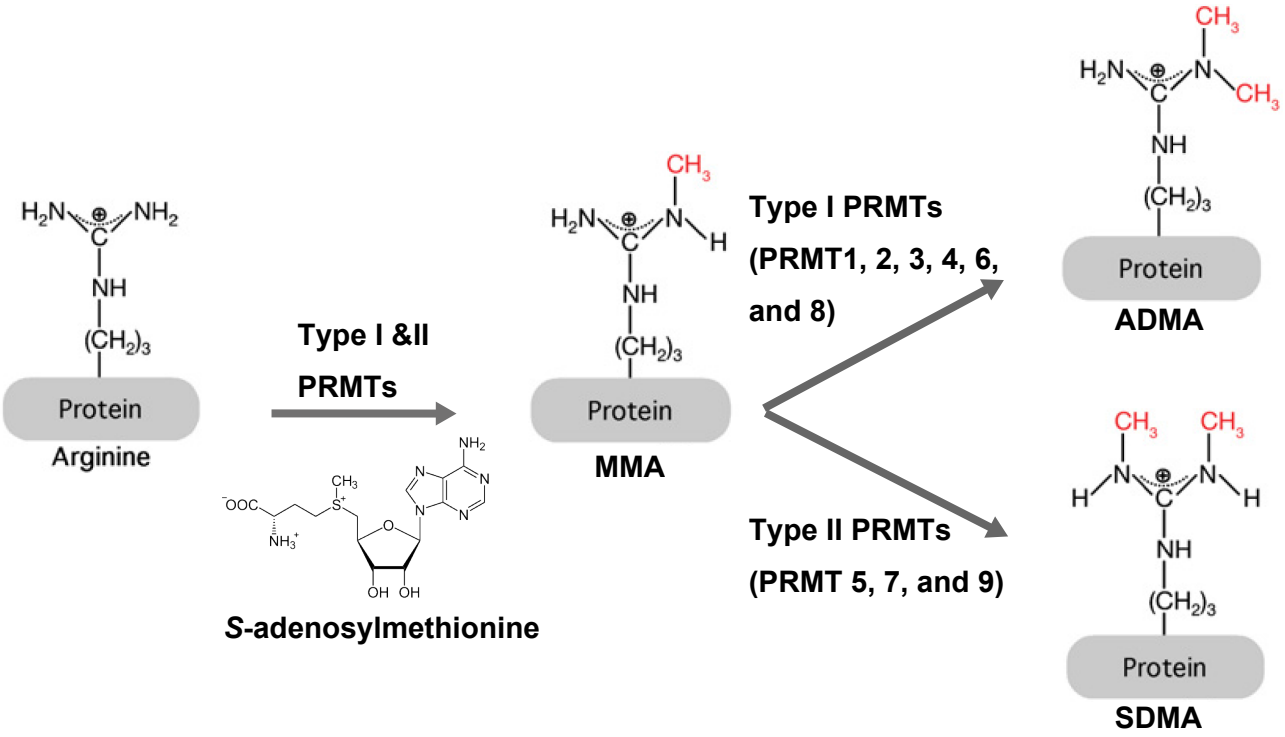

Fig. I-2. Protein arginine methyltransferases (PRMTs)

Protein arginine methylation is catalyzed by a family of enzyme called protein arginine methyltransferases (PRMTs). PRMT1-9 are categorized into two types, type I and II, depending on the modes of methylation. PRMTs form monomethyl arginine (MMA) and asymmetric dimethyl arginine (ADMA) or symmetric dimethyl arginine (SDMA) by transferring methyl groups from a methyl donor, *S*-adenosylmethionine.

Chapter II.

PRMT1 in the central nervous system is essential for development and oligodendrocyte lineage progression

Summary

Protein arginine methyltransferase 1 (PRMT1) is involved in cell proliferation, DNA damage response, and transcriptional regulation. While PRMT1 is extensively expressed in the central nervous system (CNS) at embryonic and perinatal stages, the physiological role of PRMT1 was poorly understood. Here, to investigate the primary function of PRMT1 in the CNS, I generated CNS-specific PRMT1 knockout mice by Cre-loxP system. These mice exhibited post-natal growth retardation with tremors and most of them died in two weeks after birth. Brain histological analyses revealed the prominent cell reduction in the white matter tracts of the mutant mice. Furthermore, ultrastructural analysis demonstrated that myelin sheath was almost completely ablated in the CNS of these animals. In agreement with hypomyelination, I also observed that most major myelin proteins including MBP, CNPase, and MAG were dramatically decreased, although neuronal and astrocytic markers were preserved in the brain of CNS-specific PRMT1 knockout mice. These animals had reduced number of $OLIG2^{+}$ oligodendrocyte lineage cells in the white matter. I found that expressions of transcription factors essential for oligodendrocyte specification and further maturation were significantly suppressed in the brain of the mutant mice. These findings provide

evidence that PRMT1 is required for CNS development, especially for oligodendrocyte maturation processes.

Introduction

CNS development is achieved by proliferation of progenitor cells followed by the transition from a proliferative state to differentiation. This process is considered to be tightly regulated at multiple levels such as gene transcription, translation, and protein modification. In the oligodendrocyte lineage, transcription factors are known to determine cell fate and timing of differentiation by inducing the target genes that are critical for myelination (25-27). Moreover, emerging evidence suggests that post-translational modification of proteins is one of the important determinants for oligodendrocyte lineage progression (28). For example, phosphorylation of retinoblastoma protein by AMP-activated protein kinase is essential for cell cycle progression in neural stem cells (NSCs) and their differentiation into cell types including neurons and oligodendrocytes (29). On the other hand, a histone lysine deacetylase, SIRT1, has a role in limiting the expansion of oligodendrocyte precursor cells (OPCs) (30). However, there is no *in vivo* evidence for the involvement of methylation enzymes in oligodendrocyte development and myelination. Protein arginine methylation is now widely accepted as one of the major post-translational modifications observed in both histone and non-histone proteins. Protein arginine methyltransferase (PRMT) 1, one of the type I PRMTs that catalyze monomethylation and asymmetric dimethylation of proteins, regulates transcription, cell death, DNA damage responses, and signal transduction as reviewed elsewhere (13). In mammals, PRMT1 is ubiquitously expressed in various tissues (21-24). Previous studies demonstrated that

mouse embryos that lack PRMT1 were arrested in development before embryonic day 6.5, suggesting that arginine methylation by PRMT1 is crucial for early embryonic development (22). Interestingly, the distribution pattern of PRMT1 in mouse embryo has shown high expression in neural tube during embryonic stage (22). After birth, PRMT1 is still strongly expressed in the brain during the perinatal stage (31). It should be noted that PRMT5, the most characterized member of type II PRMTs that catalyze the monomethylation and symmetric dimethylation of proteins, also shows substantial expression in the brain (31). Specific deletion of PRMT5 in CNS results in postnatal lethality with extensive apoptosis of NSCs (32). In addition, Chittka *et al.* (33) have demonstrated that PRMT5 controls NSC proliferation and differentiation. These studies indicate the important role of PRMTs in the CNS; however, little is known about PRMT1 in the development of nervous tissues. Here, my results demonstrate the essential function of PRMT1 for proper organization of the CNS by using PRMT1 conditional knockout mice and highlights the crucial role in oligodendrocyte lineage.

Materials and Methods

Animals

PRMT1 knock in mice (PRMT1-KI) that carry *Prmt1*$^{tm1a(EUCOMM)Wtsi}$ allele were obtained from the European Conditional Mouse Mutagenesis (EUCOMM). For generation of *Prmt1*$^{flox/flox}$ mice, the gene-trap cassette was removed by intercrossing *β-actin-Flp* transgenic mouse [strain name: B6.SJL-Tg(ACTFLPe)9205Dym/J, stock number: 003800, The Jackson Laboratory]. *Prmt1*$^{flox/flox}$ mice are further crossed with Nestin-Cre transgenic mice [B6.Cg-Tg(Nes-cre)1Kln/J, stock number: 003771, The Jackson Laboratory] to create *Prmt1*$^{flox/flox}$; *Nes-Cre* mice.

Genotyping of mice was performed by polymerase chain reaction (PCR) using genomic DNA from tail as previously described (34). The primers were *Prmt1* forward primer (5'-GTGCTTGCCATACAAGAGATCC-3') and reverse primer (5'-ACAGCCGAGTAGCAAGGAGG-3'). The primer set amplifies 410- and 277-bp fragments for the floxed and wildtype alleles, respectively. *Nestin-Cre* transgene was amplified using (5'-ACTGAACGCTAAAGGGTTAAG-3') and (5'-GTGAAACAGCATTGCTGTCACTT-3').

All animal experiments were done in compliance with approved by the Institutional Animal Experiment Committee of the University of Tsukuba. All these experiments were conducted in accordance with the Regulations for Animal Experiments at our institution and with the Fundamental Guidelines for the Proper Conduct of Animal Experiment and Related Activities in Academic Research

Institutions under the jurisdiction of the Ministry of Education, Culture, Sports, Science and Technology of Japan.

RNA Analysis

Whole brains were harvested at post-natal day 0 (P0) or P10 and frozen in liquid nitrogen, then stored in deep freezer until use. Frozen tissues were crashed into powder with Multi Bead Shocker (Yasui Kikai Co., Osaka, Japan). From a subset of the tissue powder, brain total RNA was isolated with ISOGEN II (Nippon Gene., Ltd., Tokyo, Japan) following manufacturer's instruction. 5 mg of the total RNA were treated with RQ1 RNase-Free DNase (Promega. Co., WI), then reverse transcribed into cDNA with ReverTra Ace (Toyobo Co., Ltd., Osaka, Japan). Relative gene expression level was determined by SYBR Green-based quantitative RT-PCR (Takara Bio Inc, Shiga, Japan). Expression levels of target gene were corrected for *Gapdh* expression levels by using ΔΔCt method. The amplification efficiency of primers for each target gene was confirmed to be equal by using serial dilutions of cDNA. The primers sequences are as follows: *Olig1* (5'-CTCGCCCAGGTGTTTTGTTG-3' and 5'-TAAGTCCGAACACCGATGGC-3'), *Olig2* (5'-GAACCCCGAAAGGTGTGGAT-3' and 5'-TTCCGAATGTGAATTAGATTTGAGG-3'), *Nkx2.2* (5'-CCTTTCTACGACAGCAGCGA-3' and 5'-CCGTGCAGGGAGTATTGGAG-3'), *Sox10* (5'-GCAGAAAGCTAGCCGACCA-3' and 5'-CTTTCGTTCAGCAACCTCCAGA-3'), and *Gapdh*

(5’-TCACTGGCATGGCCTTCC-3’ and 5’-CAGGCGGCACGTCAGATC-3’).

Western blot

Brain and kidney tissue powder was prepared as described above and was homogenized in ice-cold RIPA buffer containing 20 mM Tris-HCl, 150 mM NaCl, 1 mM EDTA, 1% NP-40, 0.5% sodium deoxycholate, 0.1% sodium dodecyl sulphate, and a proteinase inhibitor cocktail (Nacalai Tesque, Inc., Kyoto, Japan). Protein extracts were centrifuged at 14,000 rpm for 15 min at 4˚C, then concentration was determined by Bio-Rad Protein Assay Dye Reagent Concentrate (Bio-Rad, CA). Quantified total protein extracts were denatured with Laemmli sample buffer added with 100 mM DTT, then subjected to 10% or 12% SDS-PAGE, and analyzed by Western blot with various antibodies, according to standard procedures. The antibodies are as follows: anti-PRMT1 (1:1000, rabbit polyclonal; #07-404, Millipore, MA), anti-MBP (1:100, goat polyclonal; #sc-13914, Santa Cruz, CA), anti-CNPase (1:1000, rabbit monoclonal; #5664, Cell Signaling, MA), anti-MAG (1:1000, rabbit monoclonal; #9043, Cell Signaling), anti-CRMP2 (1:1000, rabbit polyclonal; #9393, Cell Signaling), anti-β-III-tubulin (1:1000, rabbit monoclonal; #5568, Cell Signaling), anti-GFAP (1:1000, mouse monoclonal; #G3893, Sigma, MO), anti-asymmetric dimethyl arginine, Asym26 (1:1000, rabbit polyclonal; #13-0011, EpiCypher, NC), anti-mono-methyl arginine (R*GG) (D5A12) (1:1000, rabbit monoclonal; #8711, Cell Signaling), anti-symmetric di-methyl arginine motif (SDMA) (1:1000, rabbit monoclonal mix; #13222, Cell Signaling), anti-GAPDH (1:10000, mouse monoclonal; #05-50118,

American Research Products, MA), and anti-β-actin (1:10000, mouse monoclonal; #A5316, Sigma). Secondary antibodies are corresponding HRP-conjugated secondary antibodies. Visualization via chemiluminescent detection was performed using SuperSignal West Femto Maximum Sensitivity Substrate (Thermo Fisher Scientific, Rockford, IL). Data images were obtained from LAS-3000 (Fujifilm, Tokyo, Japan).

For primary cells, cells were lysed with ice-cold RIPA buffer and protease & phosphatase inhibitor cocktails. Protein extracts were centrifuged at 14,000 rpm for 10 min at 4˚C, then concentration was determined by Pierce BCA Protein Assay Kit (Thermo). Quantified total protein extracts were denatured with Laemmli sample buffer added with 100 mM DTT, then subjected to 4–15% Mini-PROTEAN TGX Precast Protein Gels (#4561085, BioRad), and analyzed by Western blot with various antibodies including anti-PRMT1 (1:1000, rabbit polyclonal; #07-404, Millipore, MA), anti-MBP (1:3000, rabbit polyclonal; #AM980, Millipore, MA), and anti-GAPDH (1:1000, mouse monoclonal; #MAB374, Millipore, MA). Secondary antibodies are corresponding HRP-conjugated secondary antibodies. Visualization via chemiluminescent detection was performed using SuperSignal West Femto Maximum Sensitivity Substrate (Thermo Fisher Scientific, Rockford, IL). Data images were obtained from LI-COR Odyssey Imagers (LI-COR, NE).

Histology

Mice were transcardially perfused with 4% paraformaldehyde (PFA), immersed in the same fixative for 24 hours at 4˚C, and embedded in paraffin.

Tissues were sectioned into 7-μm thickness using a rotary microtome (HM340E; Microm International GmbH, Walldorf, Germany). Brains were sectioned either midline sagittal or in coronal section at the level of the mid cerebellum and the forebrain. Spinal cord tissues were sectioned at the thoracic level with the surrounding bones. Deparaffinized sections were stained with hematoxylin and eosin (H&E). Data images were obtained using a SZ61 microscope, a BX53 microscope, and DP21 digital camera (Olympus, Tokyo, Japan). Three to five mice per each genotype were used for histological studies.

Immunohistochemistry

For immunohistochemistry, tissue sections were deparaffinized, followed by antigen-retrieval with citrate buffer (pH 6.0) and were incubated in 3% H_2O_2 for 30 min to quench an endogenous peroxidase. Sections were incubated with TSA blocking reagent (Cat. #FP1020, PerkinElmer, MA) for 30 min and each primary antibody for 1 h at room temperature. The antibodies used were as follows: anti-MBP (1:1000, goat polyclonal; #sc-13914, Santa Cruz), anti-OLIG2 (1:1000-1:2000, rabbit polyclonal; #18953, IBL, Gunma, Japan), and anti-PRMT1 (1:200, mouse monoclonal; #ab12189, Abcam). Biotinylated horse anti-goat IgG (Cat. #BA-9500, Vector Laboratories, Inc., CA), biotinylated goat anti-rabbit IgG (Cat. #BA-1000, Vector Laboratories, Inc.), or biotinylated goat anti-mouse IgG (Cat. #BA-9200, Vector Laboratories, Inc.) was incubated for 30 min, then streptavidin-HRP (Cat. #NEL750001EA, PerkinElmer) was reacted for 30 min. Signal was amplified with TSA Plus Fluorescein System or TSA

Plus Tetramethylrhodamine (TMR) System (Cat. #NEL756001KT PerkinElmer) for 10 min, followed by Hoechst counterstaining. Fluorescence images were obtained with a fluorescence microscope (BIOREVO BZ-9000, Keyence, Osaka, Japan) and Fluoview FV10i confocal laser-scanning microscope (Olympus, Tokyo, Japan). For the quantification of immunohistochemical data, three mice per each genotype were evaluated with the ImageJ software.

Transmission Electron Microscopy

For ultrastructure analysis, mice were perfused with 2% glutaraldehyde/2% PFA, then brain and spinal cord were dissected, following immersion fixation in 2.5% glutaraldehyde in 0.1 M phosphate buffer. Tissues were then processed as standard procedure, and ultrathin sections were subjected to transmission electron microscopy analysis with JEM-1400 electron microscope (JOEL, MA) at the electron microscopy facility at University of Tsukuba. For TEM analysis, multiple numbers of sections from two to three mice per each genotype were analyzed.

LC-MS/MS Analysis

Brain tissue powder was prepared as described above and was homogenized in ice-cold deionized water. Protein extracts were centrifuged at 14,000 rpm for 10 min at 4˚C, then concentration was determined by Bio-Rad DC Protein Assay (Bio-Rad, CA). Quantified total protein extracts were further precipitated with 10% trichloracetic acid (TCA) in cold acetone. The total proteins were hydrolyzed with 6 N HCl at 110˚C for 24 h. After

hydrolysis, the residues were evaporated *in vacuo*, and reconstituted in 100 μL of deionized water for the following LC-MS/MS analysis.

The LC-MS/MS analysis was performed on a Shimadzu LCMS-8050 triple quadrupole mass spectrum coupled with a Shimadzu Nexera X2 ultra-high pressure liquid chromatography (UHPLC) system (Shimadzu, Kyoto, Japan). The instrument was operated under positive electrospray ionization and multiple reaction monitoring (MRM) modes. The chromatography separation was performed with SeQuant ZIC-HILIC column, 2.1 x 150 mm, 3.5 μm (Millipore, MA) and gradient elution comprising distilled water containing 1% formic acid and 1% acetonitrile (mobile phase A) and acetonitrile containing 1% formic acid and 1% water (mobile phase B). ZIC-HILIC Guard Fitting column, 1.0 x 14 mm (Millipore, MA) was installed preceding the SeQuant ZIC-HILIC column for the sake of sample cleanup. The MS operating conditions were optimized as follows: interface voltage, 4.0 kV; interface temperature, 300˚C; desolvation line temperature, 250˚C; heating block temperature, 400˚C; drying gas (N_2); 10 $Lmin^{-1}$; nebulizing gas (N_2); 3 $Lmin^{-1}$; heating gas (air), 10 $Lmin^{-1}$; and collision-induced dissociation gas (argon), 230 kPa. For the detection of ADMA, MMA, and SDMA, the gradient program for positive ionization method started from 95% mobile phase B at 0-1 min, decreasing to 5% to 10 min and held until 14 min. The mobile phase B content was further increased to 95% at 14.10 min and stopped at 21 min with a flow rate of 0.2 mL/min. The m/z for each analyte are as follow: ADMA, 203.15 > 158.05; MMA, 189.15 > 70.15; SDMA, 203.25 > 171.95. All analyses and data processing were completed on LabSolutions V5.60 (Shimadzu Scientific

Instruments, Inc., Columbia MD). Four mice per each genotype were used for LC-MS/MS analysis.

Primary Cell Culture

All primary cell cultures were done at Dr. Anna Williams laboratory at The University of Edinburgh in accordance with regulations of the Animal (Scientific Procedures) Act under an issued UK Home Office project license. For primary culture of mouse cells, cortices from individual P6-9 mice were processed to single-cell suspensions using the gentle-MACs dissociator (Miltenyi Biotec, Bergisch Gladbach, Germany), according to the manufacturer's instructions. Mouse oligodendrocyte precursor cell (OPC) cultures were prepared from cell suspensions by immunopanning with anti–platelet-derived growth factor (PDGF) alpha receptor antibody as described previously (35-37). The immunopanned OPCs were seeded on poly-D-lysine (PDL) coated T-75 or T-150 flasks and cultured at 37°C in 7.5% CO_2. OPCs from each animal were maintained separately under proliferating conditions for 7–9 days in proliferation media composed of mouse OPC media with PDGF-AA (10 ng/mL, Peprotech, London, UK) and neurotrophin 3 (NT3) (5 ng/mL, Peprotech, London, UK). Mouse OPC media was composed of SATO media (DMEM high Glucose with Glutamax (Invitrogen #311966-021), 100 µg/mL BSA, 40 µg/mL sodium selenite (Sigma #S5261), 16 µg/mL putrescine (Sigma #P5780), 62.5 ng/mL progesterone (Sigma #P8783), 100 µg/mL apo-transferrin (Sigma #T1147)), 10% fetal bovine serum (FBS, Invitrogen), 1% penicillin/streptomycin (pen/strep, Invitrogen), 1x B27 supplement (Invitrogen #17504-044), 60 µg/mL N-acetyl-cysteine

(Sigma #A9165), 5 μg/mL Insulin (Sigma #91077C), 1:1000 Trace element B (Mediatech #99-175-CI), 1 ng/mL biotin (Sigma #B4639), and 5 mM Forskolin (Sigma #P8783). OPCs were de-adhered from flasks using TrypLE (Life Technologies, CA), counted after staining with trypan blue and then seeded on PDL coated 13 mm glass coverslips ($7x10^4$/mL/coverslip) in 4-well culture plate with the proliferation media.

For overexpression experiments, pVenus vector or Venus-mPRMT1v2 (both plasmids were kindly provided by Dr. Murata) were incubated with Lipofectamine 2000 Transfection Reagnt (Thermo Fisher Scientific) and transfected into cells according to the manufacturer's instruction. After three hours of transfection, proliferation media was changed to differentiation media to induce OPC differentiation into oligodendrocytes. Differentiation media were composed of mouse OPC media with differentiation factors including ciliary neurotrophic factor (CNTF) (10 ng/mL, Peprotech, London, UK), triiodothyronine (T3) (50 μg/mL, Sigma), and NT3 (5 ng/mL) and were promoted to differentiate by changing media everyday.

Rat OPC isolation and culture was conducted as previously reported (36). Briefly, OPCs were isolated from pooled P0-P2 Sprague-Dawley neonatal rat cerebral cortices. Cortices were isolated, meninges removed, minced, and cells were dissociated for 60 min at 37˚C with 1.2 U/mL papain (Worthington), 0.1 mg/mL L-cysteine (Sigma) and 0.40 mg/mL DNase I (Sigma). The resulting mixed glial cultures were plated onto PDL coated flasks and cultured at 37˚C in 7.5% CO2 in DMEM (Invitrogen 41966029), 10% fetal bovine serum (FBS, Invitrogen) and 1% penicillin/streptomycin (pen/strep, Invitrogen). Mixed glial cultures were separated after 10 days by mechanical shaking at

240 rpm for 1 h to remove microglia followed by additional 18 h shaking. Cells collected were plated onto petri dishes 20 min for differential adhesion to further remove microglia and astrocytes. The enriched OPCs were collected and plated on PDL coated 13 mm glass coverslips ($7x10^4$ cells/mL/coverslip) in 24-well culture plate with rat OPC SATO media. To keep proliferated rat OPCs were cultured with PDGF-AA (10 ng/mL) and FGF (10 ng/mL). To induce differentiation, these growth factors were removed from media and were cultured for up to five days to see oligodendrocytes develop myelin membrane.

Immunocytochemistry

Cells were washed once with phosphate buffered saline, pH 7.4 (PBS), fixed in 4% PFA, followed by PBS washes, and blocking and permeabilization in 0.1% TritonX-100 in PBS for 1 h at room temperature. Primary antibodies were diluted in the blocking solution, as indicated below, and incubated overnight at 4˚C. Primary antibodies used were: rabbit anti-NG2 (1:100, #AB5320, Millipore), chicken anti-GFP (1:500, #ab13970, Abcam), rat anti-MBP (1:300, #MCA409S, BioRad), mouse anti-O4 (1:2,000, Immunosolv, UK), and rabbit anti-PRMT1 (1:200, #07-404, Millipore). Cells were washed in PBS again and incubated for 1 h with AlexaFluor 350, 488, 568, or 647 conjugated secondary antibodies against rat, rabbit, mouse, or chicken (Invitrogen), used at a 1:250 or 1:1000 dilutions. Cells were washed again and mounted with Fluoromount G (Southern Biotech) with cover glass onto glass slides. Fluorescence images were obtained with Fluoview FV10i confocal laser-scanning microscope. For

the quantification of immunocystochemical data, only GFP positive cells were considered as transfected and expressed exogenous Venus protein, and were counted. Three 20x fields per coverslip from three to four coverslips per each condition were evaluated with the ImageJ software.

Results

PRMT1 Deletion in the CNS Causes Post-natal Lethality of Mice

To address the primary function of PRMT1 in the CNS, I produced CNS-specific PRMT1 knockout mice. *Prmt1*$^{KI/KI}$ mice were mated with *β-actin-Flp* transgenic mice to produce *Prmt1*$^{flox/flox}$ mice. In *Prmt1*^{flox} allele, exon 4 and 5, which encode a part of methyltransferase domains, are flanked by the two loxP sites enabling me to obtain functional null allele by Cre-mediated recombination. *Prmt1*$^{flox/flox}$ mice were crossed to animals expressing *Nestin-Cre* (*Nes-Cre*) to generate *Prmt1*$^{flox/flox}$*; Nes-Cre* animals (referred to as CKO in figures) (Fig. II-1, *A* and *B*) (38). In the whole brain lysates from embryos and post-natal mice, I confirmed the marked reduction of PRMT1 protein level by Western blot, whereas other tissues such as kidney expressed PRMT1 normally (Fig. II-1, *C* and *D*). In the brain, there was faintly remaining expression that is possibly from Nestin-Cre inactive components such as vessels or from incomplete recombination at the *Prmt1* gene locus.

The number of *Prmt1*$^{flox/flox}$*; Nes-Cre* animals were born close to the normal Mendelian ratio (Table 1) and appeared to be normal at birth. Their body weights were similar when compared to other littermates including *Prmt1*$^{flox/flox}$, *Prmt1*$^{flox/wt}$*; Nes-Cre*, and *Prmt1*$^{flox/wt}$ on the day of birth (Fig. II-1*E*). However, *Prmt1*$^{flox/flox}$*; Nes-Cre* animals displayed post-natal lethality and all mice died within 17 days after birth (Fig. II-1*F*).

Loss of PRMT1 in the CNS Results in Dynamic Change in Methyl Arginine Levels

in the Brain

Since PRMT1 catalyzes the formation of asymmetric dimethyl arginine (ADMA) in proteins, I performed acid hydrolysis of proteins from the whole brain tissue and measured the level of ADMA by LC-MS/MS. As shown in Fig. II-2*A*, ADMA levels in *Prmt1*$^{flox/flox}$*; Nes-Cre* mice were almost two-fold lower than that of *Prmt1*$^{flox/flox}$ mice. The decrease of tissue ADMA levels was also confirmed by Western blot using an antibody against ADMA (Fig. II-2*B*). Altogether, these results implicate that PRMT1 serves as a major methyltransferase that catalyzes the formation of ADMA in the mouse brain.

Deletion of PRMT1 in mouse embryonic fibroblasts (MEFs) induces upregulation of monomethyl arginine (MMA) and symmetric dimethyl arginine (SDMA) levels (39). I therefore examined the level of MMA and SDMA in the brain tissues by LC-MS/MS and Western blot. Both MMA and SDMA levels showed dramatic elevation in *Prmt1*$^{flox/flox}$*; Nes-Cre* pups compared with *Prmt1*$^{flox/flox}$ mice (Fig. II-2, *A* and *B*), suggesting the loss of PRMT1 actually affected the status of protein arginine methylation on multiple proteins in agreement with the previous *in vitro* work.

Growth Retardation and Reduced Nuclei in the White Matter in *Prmt1*$^{flox/flox}$*; Nes-Cre* Mice

I then characterized the brain morphology and the behavioral outcomes to clarify the effect of PRMT1 deletion in the CNS. *Prmt1*$^{flox/flox}$*; Nes-Cre* animals started to show growth retardation at around post-natal day 4 (P4) (Fig. II-3*A*) and their body

size became apparently small at P10 with reduced brain size and weight and seemingly emaciated (Fig. II-3, *B* and *C*). Histological analysis of nervous tissues revealed that all white matter tracts in the CNS including corpus callosum, fimbria, anterior commissure, and spinal white matter had reduced number of nuclei stained by hematoxylin. Although nuclei in both white and gray matter areas were decreased in the spinal cords, more prominent difference was observed in the white matter part (Fig. II-4). Considering that white matter tracts consist of predominantly oligodendrocytes and much less number of nuclei of neuron and astrocytes, the above data imply that cellular organizations are changed in the CNS tissues of *Prmt1*$^{flox/flox}$*; Nes-Cre* mice.

Behavioral Deficits in *Prmt1*$^{flox/flox}$*; Nes-Cre* Mice

Remarkably, *Prmt1*$^{flox/flox}$*; Nes-Cre* mice manifested ataxic behavior and tremors, which became evident after one week of birth (Video 1). This behavioral defect is reminiscent of mouse models with hypomyelination such as myelin-deficient shiverer mice (*shi*) (40) or quaking viable mice (qk^v) (41, 42). The similar behavioral phenotype in *Prmt1*$^{flox/flox}$*; Nes-Cre* animals prompted me to analyze the level of myelination in the CNS.

Severe Hypomyelination and Dramatic Decrease of Mature Oligodendrocytes in *Prmt1*$^{flox/flox}$*; Nes-Cre* Mice

Myelin is a multilamellar structure that is formed by mature oligodendrocytes and wrapping around a number of axons allowing rapid saltatory conduction in the CNS.

I evaluated myelin formation at P10 because myelination actively occurs from the first week to the third week after birth in rodents (43) and I had limitation to obtain tissues after the second week due to the short life span of *Prmt1*$^{flox/flox}$*; Nes-Cre* mice. To examine ultrastructure of myelin sheaths, I performed transmission electron microscope (TEM) analysis, and confirmed that a substantial number of axons were myelinated in *Prmt1*$^{flox/flox}$ mice spinal cord and brain. By contrast, in the spinal cord, only a few axons were myelinated in *Prmt1*$^{flox/flox}$*; Nes-Cre* mice. Similarly, myelin structure was totally ablated in the corpus callosum of *Prmt1*$^{flox/flox}$*; Nes-Cre* mice (Fig. II-5*A*). Thus, TEM analysis clearly showed hypomyelination in the CNS tissues of *Prmt1*$^{flox/flox}$*; Nes-Cre* mice.

Mature oligodendrocytes produce myelin specific proteins such as myelin basic protein (MBP), 2',3'-cyclic-nucleotide 3'-phosphodiesterase (CNPase), and myelin-associated glycoprotein (MAG) (44, 45), allowing compact myelin formation and axon stability. These myelin protein levels were dramatically decreased in the *Prmt1*$^{flox/flox}$*; Nes-Cre* mice compared to *Prmt1*$^{flox/flox}$ mice as confirmed by Western blot. On the other hand, neuronal and astrocytic markers were observed in the same level between *Prmt1*$^{flox/flox}$ and *Prmt1*$^{flox/flox}$*; Nes-Cre* brain (Fig. II-5*B*). Consistent with those findings, immunohistochemical analysis revealed that near-complete loss of MBP positive signals in whole brain regions including the white matter tracts in the corpus callosum, striatum, cerebellum, and the spinal cord in *Prmt1*$^{flox/flox}$*; Nes-Cre* mice (Fig. II-5*C*), although there were still intense signals in the spinal roots that are composed of peripheral nerves (an inset in Fig. II-5*C*). Collectively, these data demonstrated

extensive dysmyelination caused by the dramatic reduction of mature oligodendrocytes in the CNS tissues of *Prmt1*$^{flox/flox}$*; Nes-Cre* mice.

Oligodendrocyte Lineage Cells Were Reduced in *Prmt1*$^{flox/flox}$*; Nes-Cre* Mice

Myelinating mature oligodendrocytes are developmentally derived from highly proliferative OPCs that are originally from NSCs. OPCs develop into premyelinating oligodendrocyte, and terminally differentiate into mature myelinating oligodendrocytes (25). Since I observed near-complete loss of mature oligodendrocytes, I investigated whether OPCs and premyelinating oligodendrocytes are also absent by immunohistochemistry for OLIG2, which represents all oligodendrocyte lineage cells, and MBP which marks only mature oligodendrocytes. To exclude mature oligodendrocytes from all OLIG2^{+} cells, I counted the number of OLIG2^{+}MBP^{-} cells in the striatum and assumed them as OPCs or immature oligodendrocytes. I detected reduced number of OLIG2^{+} cells not only in the striatum but also in the cerebellum and the spinal cord in *Prmt1*$^{flox/flox}$*; Nes-Cre* mice, suggesting that oligodendrocyte lineage progression is not completely but partially suppressed (Upper panels of Fig. II-6*A* and II-6*B*). Furthermore, *Prmt1*$^{flox/flox}$*; Nes-Cre* mice had less than half the number of OLIG2^{+}MBP^{-} cells relative to *Prmt1*$^{flox/flox}$ mice in the striatum (Lower panels of Fig. II-6*A* and *the graph*). Therefore, these results show that OPCs and/or premyelinating oligodendrocytes are dramatically reduced in PRMT1 mutant mice.

Oligodendrocyte development is mainly promoted by several key transcription factors and many of them belong to basic-helix-loop-helix (bHLH) protein family,

homeodomain proteins, and high-mobility-group (HMG) domain proteins. Especially, *Olig1*, *Olig2*, *Nkx2.2*, and *Sox10* are well characterized as positive regulators of oligodendrocyte differentiation (45-49).

While *Olig2* and *Olig1* a necessary for specification of oligodendrocyte lineage cells from NSCs, *Nkx2.2* and *Sox10* serve as modulator of the later differentiation for example by adjusting the timing of oligodendrocyte differentiation (27). Quantitative RT-PCR analysis revealed a significant reduction of these genes in *Prmt1*$^{flox/flox}$*; Nes-Cre* brain at birth. Moreover, the differences became more evident at P10 when oligodendrocyte maturation is most activated in normal condition (Fig. II-6*C*). A previous report (31) demonstrated that the inhibitory transcription factors including *Id2/4* were upregulated upon knockdown of PRMT5 in rat primary OPCs and C6 glioma cell line. mRNA levels of these factors were not changed in the brain of *Prmt1*$^{flox/flox}$*; Nes-Cre* mice compared to *Prmt1*$^{flox/flox}$ mice (Fig. II-6*C*). Thus, the downregulation of positive regulators of differentiation may explain the reason for suppressed differentiation of oligodendrocyte and/or reduced number of OLIG2^{+} cells. Taken together, these data indicated that PRMT1 is a key regulator of oligodendrocyte differentiation during the CNS development.

PRMT1 is expressed by oligodendrocyte lineage cells *in vitro* and *in vivo*

The above data raised a question whether PRMT1 regulates oligodendrocyte development by cell-intrinsic manner. To test this is possible, first, immunohistochemical and immunocytochemical analyses were conducted to understand

a profile of PRMT1 expression in oligodendroglia. A number of PRMT1 signals were detected in the cell nucleus in the cerebellar white matter of *Prmt1*$^{flox/flox}$ animals at P4, and these were completely absent in the same region of *Prmt1*$^{flox/flox}$*; Nes-Cre* mice (Fig. II-7*A*). In addition, some of the PRMT1^{+} nuclei were also labeled with OLIG2, suggesting that PRMT1 is expressed by oligodendrocyte lineage cells (Fig. II-7*A, arrowheads*). It should be noted that the OLIG2^{+} cells were apparently decreased in the mutant animals already at P4, consistent with the result obtained at P10 (Fig. II-6*B*).

To know PRMT1 is expressed at which stage of differentiation, its expression was tested by *in vitro* cell differentiation assay. In mouse proliferating OPCs in a condition with most cells expressed an OPC marker NG2, PRMT1 was strongly expressed in the nucleus and was merged with OLIG2 (Fig.II-7*B*). This nuclear localization of PRMT1 was further confirmed in rat differentiated oligodendrocytes, which was also in agreement with the *in vivo* data (Fig. II-7*, A-C*). PRMT1 signals were not detected at the processes of OPCs and myelin membrane (Fig.II-7*C*). It is of note that some signals of PRMT1 were also detected in the cell body around nucleus in cultured OPCs/OLs (Fig. II-7*B* and II-*7C*), indicating that PRMT1 does not exclusively reside in the nucleus but partly exists in the cytoplasm. In addition, Western blotting showed PRMT1 expression by oligodendroglia at all stages of differentiation. It showed the strongest expression in OPCs and was gradually decreased as cells differentiate to MBP-expressing mature oligodendrocytes (Fig.II-7*D*). This trend was consistent with the previously reported RNA-seq. database (50) and both findings indicate that PRMT1 is more important for the earlier stage of development rather than the later stages

throughout oligodendrocyte development.

Overexpression of PRMT1 in primary OPCs did not accelerate oligodendrocyte differentiation

As the above *in vivo* data suggested the possibility that PRMT1 acts as a positive regulator of oligodendrocyte differentiation, I sought to determine whether PRMT1 overexpression could increase the rate of OPC differentiation into mature oligodendrocyte. To examine this point primary mouse OPCs were transfected with Venus-tagged PRMT1 or control Venus vector and the rate of differentiation was evaluated by immunocytochemical detection of OL stage-specific markers. Approximately 20-40% of cells were transfected and expressed Venus-derived fluorescence which was also detected by GFP immunolabeling in both PRMT1 or Control transfected cells (data not shown). Cultured mouse OPCs are known to express stage-specific proteins as they differentiate and elaborate myelin membranes (51). NG2, O4, and MBP are well-characterized markers to label OPC, immature OL, and mature myelinating OL, respectively (51). Although protein level from the transfected plasmids would be higher at 72 hours of transfection than the earlier time point, the majority of the cells were dead due to the weakness of primary mouse OPCs (data not shown). So differentiation was evaluated at 24, 48, and 56 hours after transfection. Cells transfected both plasmids were morphologically differentiated and expressed stage-dependent cell markers (data not shown), however there was no difference in the rate of differentiation between PRMT1 or Control transfected cells (Table 2). These data indicate that PRMT1

is not essential for OL differentiation potential or the endogenous level of PRMT1 is sufficient to maintain the normal level of OL differentiation.

Discussion

The aim of this study was to clarify the physiological role of PRMT1 in the CNS. CNS-specific PRMT1 knockout mice exhibited morphological abnormalities of the brain and many of them died within two weeks after birth. Since they displayed severe tremors, we analyzed CNS myelination and found that they exhibit nearly complete loss of myelinating oligodendrocytes. In addition, oligodendrocyte lineages were significantly decreased in CNS tissues. These results suggest that PRMT1 plays a crucial role in oligodendrocyte differentiation and CNS development.

I showed that MBP^+ mature oligodendrocytes were almost lost in CNS-specific PRMT1 knockout mice. Furthermore, I found only a small number of $OLIG2^+$ oligodendrocyte lineages and $OLIG2^+MBP^-$ OPCs/immature oligodendrocytes in the mutant animals. At least two possibilities may explain the decrease of these cells in the CNS. Firstly, it could be caused by decreased level of OPCs proliferation. OPCs increase their number before differentiation into postmitotic oligodendrocytes (52). Thus, failure of this process will directly affect the number of $OLIG2^+$ oligodendrocyte lineage cells. It is also likely that increased cell death of OPCs affected lower cell number for example by cell cycle deregulation (29). By contrast, an alternative explanation is that an altered differentiation potential of NSCs. In other words, PRMT1-deleted NSCs might have low ability to differentiate into OPCs. From these possible mechanisms, PRMT1 may modulate oligodendrocyte development not only at terminal differentiation/myelination but also at the earlier point of differentiation.

In the present study, I found that PRMT1 plays a critical role in oligodendrocyte lineage progression. A previous study has shown that PRMT5 knockdown in C6 rat glioma cells and primary rat OPCs led to repressed maturation of oligodendrocyte, indicating that PRMT5 is important for oligodendrocyte differentiation (31). These studies suggest that both PRMT1 and PRMT5 positively regulate oligodendrocyte development. It is of note that PRMT1 and PRMT5 show distinct temporal expression patterns in the brain (31). While PRMT1 shows a strong expression at birth and then decreases as mice grow, PRMT5 gradually increases after P11 and peaked at adult stage (31). Given these distinct expression patterns, it is likely that PRMT1 and PRMT5 control oligodendrocyte maturation in different time points during CNS development.

Oligodendrocyte differentiation is tightly regulated by various key transcription factors. Several reports have shown that their interplay is important for proper oligodendrocyte development (53-55). *Id2* and *Id4*, which are known oligodendrocyte differentiation inhibitors, were upregulated upon knockdown of PRMT5 in rat primary OPCs and C6 glioma cell line (31). In C6 glioma cells, PRMT5 symmetrically dimethylated arginine 3 of histone H4 (H4R3) to lead repression of these genes (31). In general, compared that symmetric dimethylation of H4R3 (H4R3me2s) causes transcriptional repression (56), asymmetric dimethylation of H4R3 (H4R3me2a) by PRMT1 induces gene transcriptional activation by permitting subsequent acetylation of chromatin, leading to establishment of active state of chromatin (16, 17). In addition, growing number of evidence suggest that PRMT1 positively regulates gene expression

by methylating transcriptional factors and transcription coactivators (18-20). In light of these findings, PRMT1 may regulate the function of key transcription factors including *Olig2*, *Sox10*, or *Nkx2.2.* by methylation and modulate the timing of oligodendroglial maturation. Interestingly, while these positive regulators of differentiation were clearly decreased (Fig. II-6*C*), differentiation inhibitors including *Id2* and *Id4* were not changed in the brain of CNS-specific PRMT1 knockout mice at P0 and P10 (Fig. II-6*C*). This observation also supports our novel hypothetical view that PRMT1 and PRMT5 have different regulatory mechanisms of oligodendrocyte differentiation.

CNS-specific PRMT1 knockout neonates exhibited small body size and consequently most of them died in two weeks. A famous hypomyelination model, shiverer mouse (*shi*) has autosomal recessive mutation in *Mbp* gene. *Shi* mutant is seemingly normal at birth but develop tremors later, and die within five months (40). Compared to *shi*, our model has shorter life span and is remarkably small and emaciated. Since both models show nearly complete absence of myelination, the difference in life span and growth may not be explained just by defective myelination. In many cases, gene deletion of positive regulator of oligodendrocyte differentiation factors results in perinatal death. For instance, Sox10 deficient mice show defective oligodendrocyte development and die either before or at birth (49, 57). Olig2 null mutant present complete absence of oligodendrocyte lineages and die at the day of birth (46, 47). In the course of oligodendrocyte development, *Olig2* and *Sox10* regulate initial and later differentiation compared that *Mbp* is crucial for establishing myelin structure. Considering that these proteins temporally regulate oligodendrocyte development,

PRMT1 may be important for cell commitment to oligodendrocyte lineage before myelination. If so, it is reasonable that our model dies earlier than *shi* mutant.

This possibility is also supported by the analysis of PRMT1 expression pattern in OPCs/oligodendrocytes in culture, as it is expressed by all the stages of development but higher at the steps before myelination. Moreover, PRMT1 was expressed at relatively stronger level in the nucleus in these cells than other part of the cells, which would enable PRMT1 to cooperate with nuclear proteins for cell differentiation such as transcription factors or histone proteins. Although overexpression of PRMT1 in primary OPCs did not accelerate the rate of differentiation, this is likely because the endogenous PRMT1 could fully methylate its critical substrate for cell differentiation. In this case, the amount of substrate but not the level of PRMT1 would be rate-limiting.

I could not perform detailed analysis of other CNS cell types including neuron, astrocyte, and microglia, except Western blotting showing neuronal and astrocyte markers expressed at the same level between control and CNS-specific PRMT1 knockout mice. So some phenotypes observed in CNS-specific PRMT1 knockout mice may be attributed to further deficiency in other cell lineages besides OPC/oligodendrocytes. It should be noted that a recent paper demonstrated that PRMT1 methylates KCNQ potassium channels on the surface of neurons and positively regulates the channel activity, thereby haploinsufficiency of PRMT1 in mice results in mild epileptic seizures (58). If this is also the case in neonatal mice, it is probable that shivering phenotype observed in postnatal CNS-specific PRMT1 knockout mice is

caused not only by the defective myelination but also by dysfunctional neuronal activity. Further analysis will be required to reveal the role of PRMT1 in neuronal function.

In conclusion, this study provides evidence that PRMT1 is critical for oligodendrocyte lineage progression. In addition, decreased number of oligodendrocyte lineage cells suggest that PRMT1 is a key regulator for cell development of NSCs and OPCs/immature oligodendrocytes in the CNS (Fig. II-8). Finally, the present genetic model will afford next challenges on analyses of additional functions of PRMT1 in the CNS.

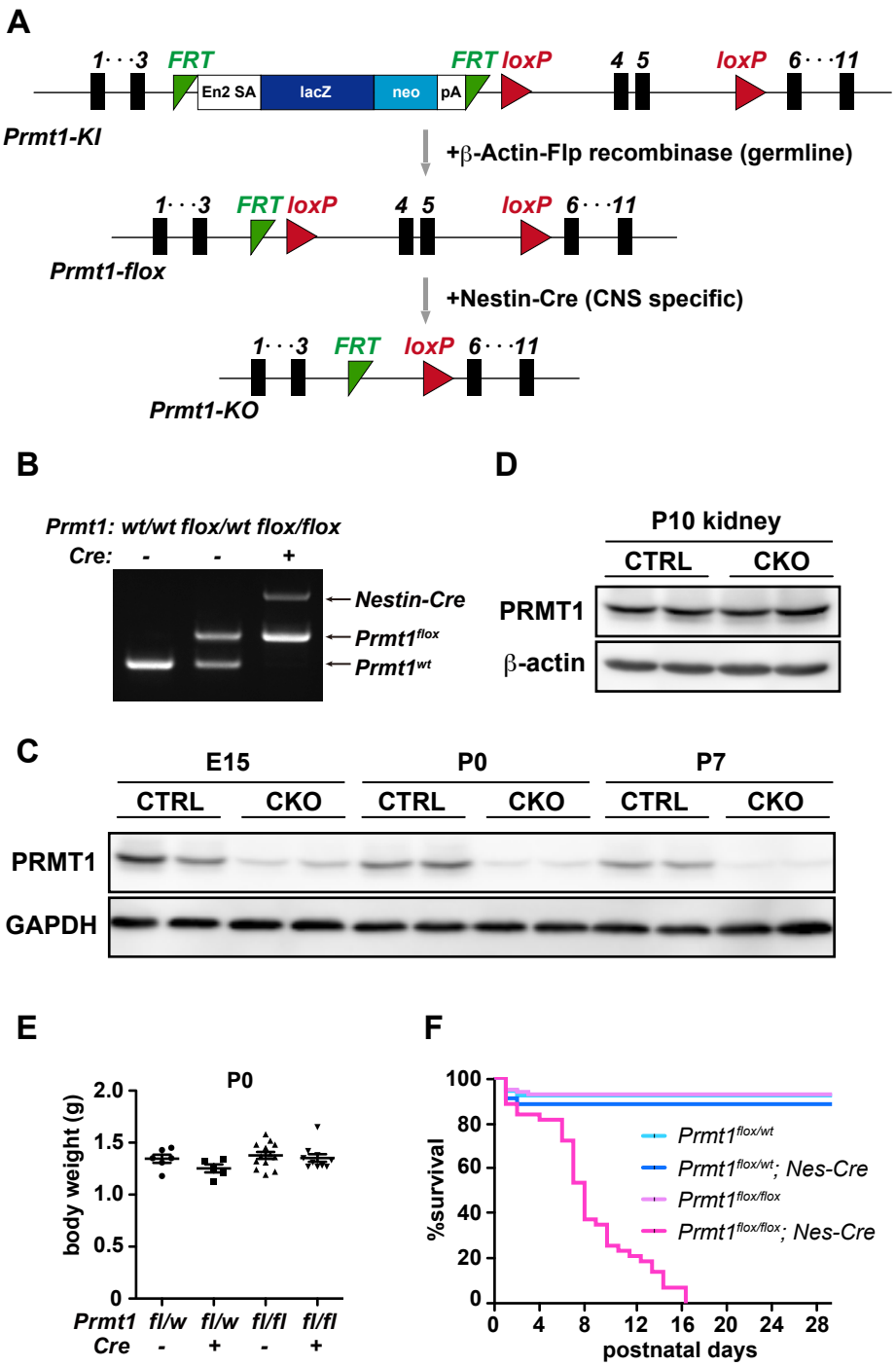

Fig. II-1. PRMT1 deletion in the CNS causes post-natal lethality of mice

(A) Schematic view of Prmt1 gene targeting design used in this study. (Figure was adapted from IMPC website: http://www.mousephenotype.org.) Black filled squares represent exons and grey arrows indicate mating with other transgenic mice for gene recombination. (B) Genotyping PCR for *Prmt1* allele and *Nestin-Cre* (*Nes-Cre*) allele. (C) Western blot showing developmental time course of PRMT1 protein expression in the brain of $Prmt1^{flox/flox}$ (hereafter, CTRL) and $Prmt1^{flox/flox}$*; Nes-Cre* (hereafter, CKO) mice. (D) Western blot showing PRMT1 protein expression in the kidney of CTRL and CKO mice at P10. (E) Body weights of $Prmt1^{flox/wt}$ (n=6), $Prmt1^{flox/wt}$*; Nes-Cre* (n=5), $Prmt1^{flox/flox}$ (n=13), and $Prmt1^{flox/flox}$*; Nes-Cre* mice (n=10) at P0. The points in the graph show individual data sets from each animal with lines and error bars indicating mean ± SEM. (F) Kaplan-Meier survival analysis of $Prmt1^{flox/flox}$ (n=106), $Prmt1^{flox/wt}$*; Nes-Cre* (n=88), $Prmt1^{flox/wt}$ (n=57), and $Prmt1^{flox/flox}$*; Nes-Cre* mice (n=47).

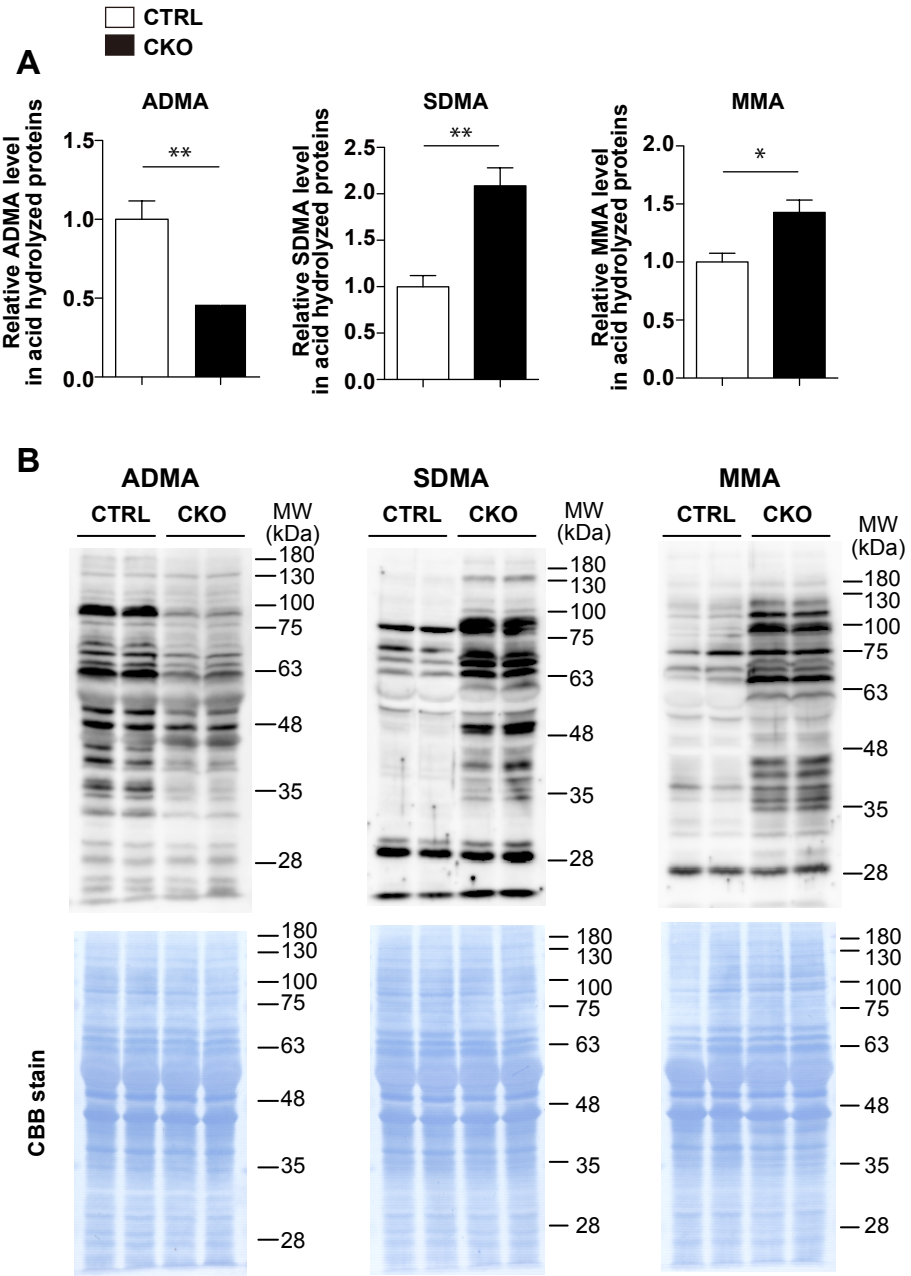

Fig. II-2. Loss of PRMT1 in the CNS results in dynamic change in methyl arginine levels in the brain

(A) ADMA, SDMA, and MMA levels in the brain of CTRL and CKO mice were quantitated by LC-MS/MS at post-natal day 10 (hereafter, P10). Data were obtained from acid hydrolysate of proteins from each brain sample. The data shown are mean ± SEM and analyzed by a two-tailed Student's t test. n=4 per each genotype.*$P < 0.05$, ** $P < 0.01$ (B) ADMA, SDMA, and MMA levels in the whole brains were detected by Western blot (upper panels) at P10, and loaded protein samples on membrane were confirmed to be equal by CBB stain (lower panels). Molecular weight (MW) markers are indicated in kilodaltons (kDa) on the right of each panel.

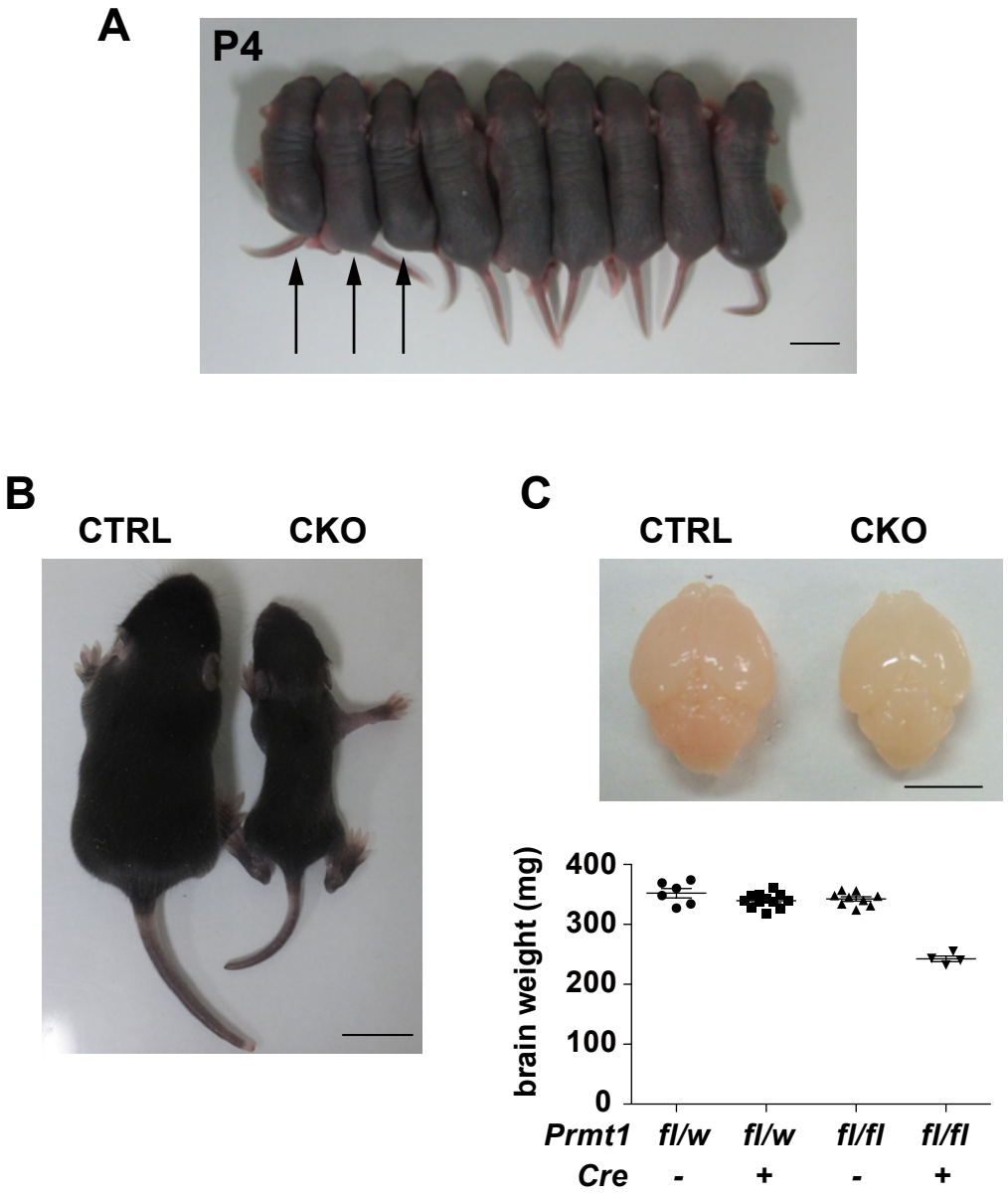

Fig. II-3. Growth retardation in *Prmt1*$^{flox/flox}$*; Nes-Cre* mice

(A) Photograph of representative CKO mice and other littermate controls at P4. The left three pups (arrows) are confirmed to be *Prmt1*$^{flox/flox}$*; Nes-Cre* by PCR analysis and smaller than other littermates. Other control littermates include *Prmt1*$^{flox/flox}$ and *Prmt1*$^{flox/wt}$*; Nes-Cre* mice. Scale bar represents 1 cm. (B) Representative example of body sizes of CTRL and CKO mice at P10. Scale bar represents 1 cm. (C) Upper panel shows the representative brain size and the lower graph shows the fresh brain weights from littermate controls at P10. Scale bar represents 5 mm. The points in the graph show individual data sets from each animal with lines and error bars indicating mean ± SEM. n=4-12 per each genotype.

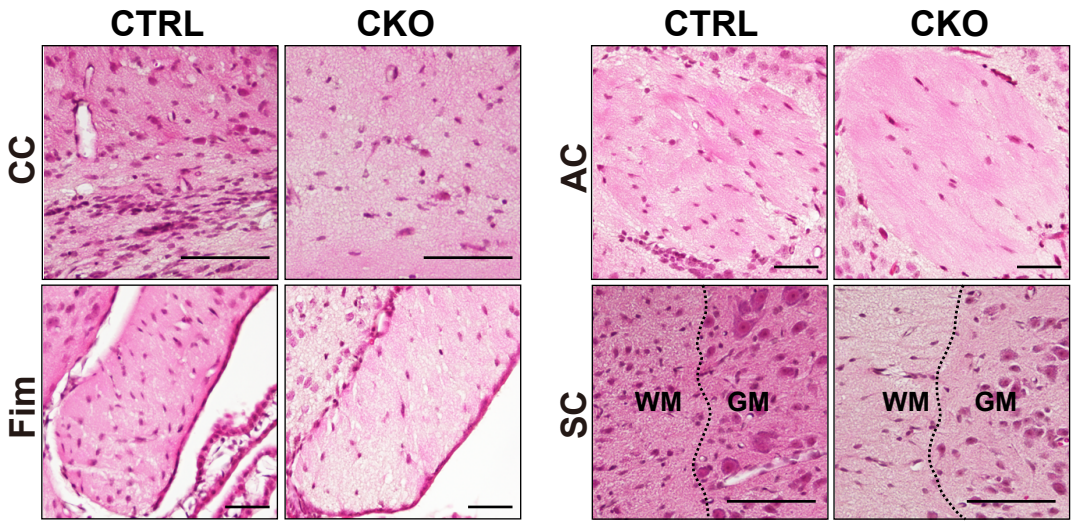

Fig. II-4. Histological abnormalities of the white matter parts in *Prmt1*$^{flox/flox}$*; Nes-Cre* mice

Hematoxylin and eosin staining images of brains and spinal cords from CTRL and CKO mice at P10 obtained from coronal sections of tissues. CC, corpus callosum; Fim, Fimbria; AC, anterior commissure; SC, spinal cord. Dotted lines represent the boundary of white matter (WM) and gray matter (GM). Scale bars represent 100 μm.

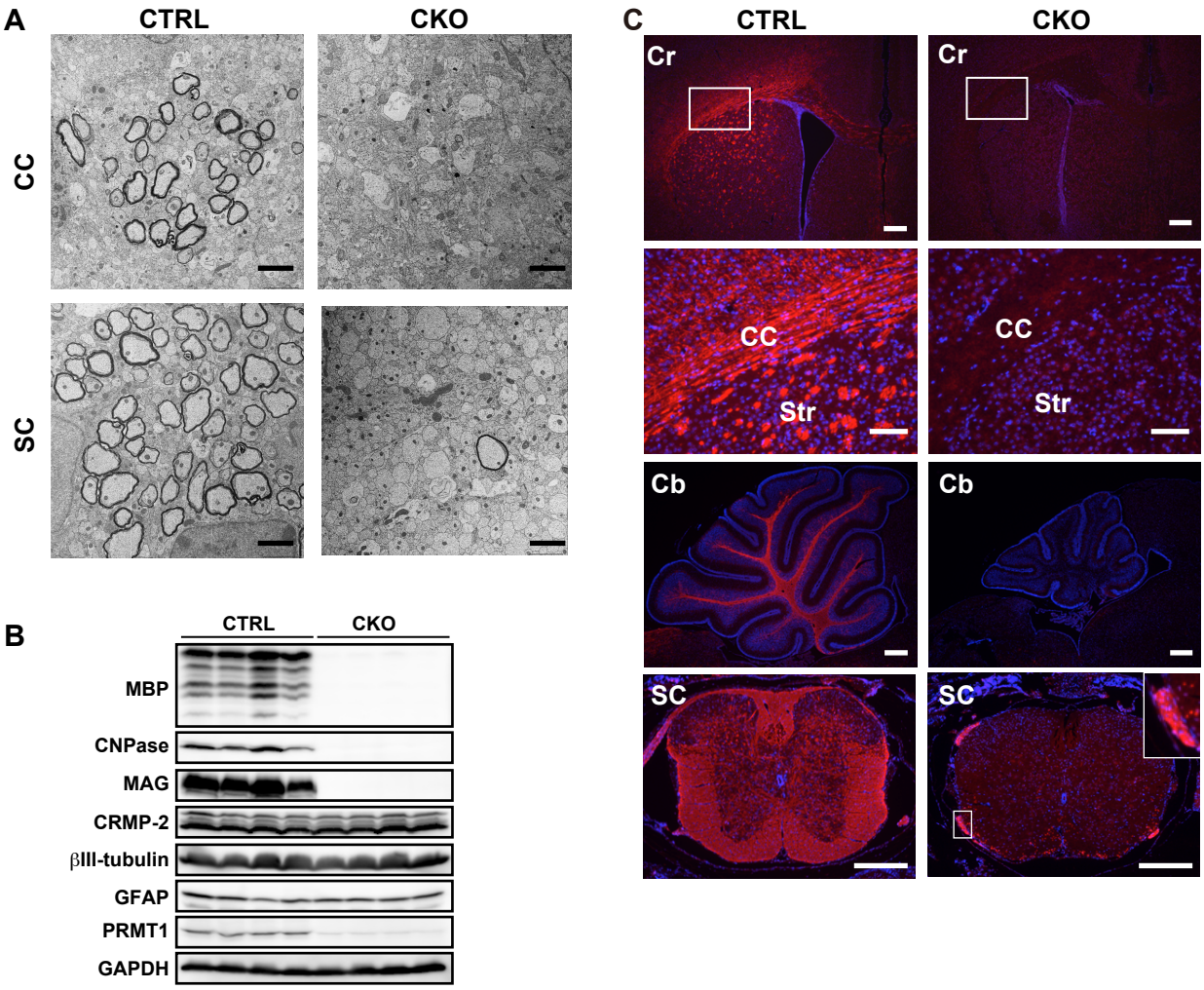

Fig. II-5. Severe hypomyelination and dramatic decrease of mature oligodendrocytes in *Prmt1*$^{flox/flox}$*; Nes-Cre* mice

(A) Representative electron micrograph images of corpus callosum (CC) and SC of CTRL and CKO mice at P10. (B) Western blot of MBP, CNPase, MAG, CRMP-2, βIII-tubulin, GFAP, and PRMT1 expression in the brain of CTRL and CKO mice at P10. (C) Immunostaining images of MBP (red) with nuclear counterstain Hoechst (blue) in the cerebrum (Cr), the cerebellum (Cb), and the spinal cord (SC) of CTRL and CKO mice at P10. White squared region (CC) is magnified in the second columns. White squared region (SC) is magnified and shown in the inset. Scale bars represent 2 μm in (A) and 300 μm in Cr, Cb, and SC in (C), and 100 μm in magnified images of CC in (C).

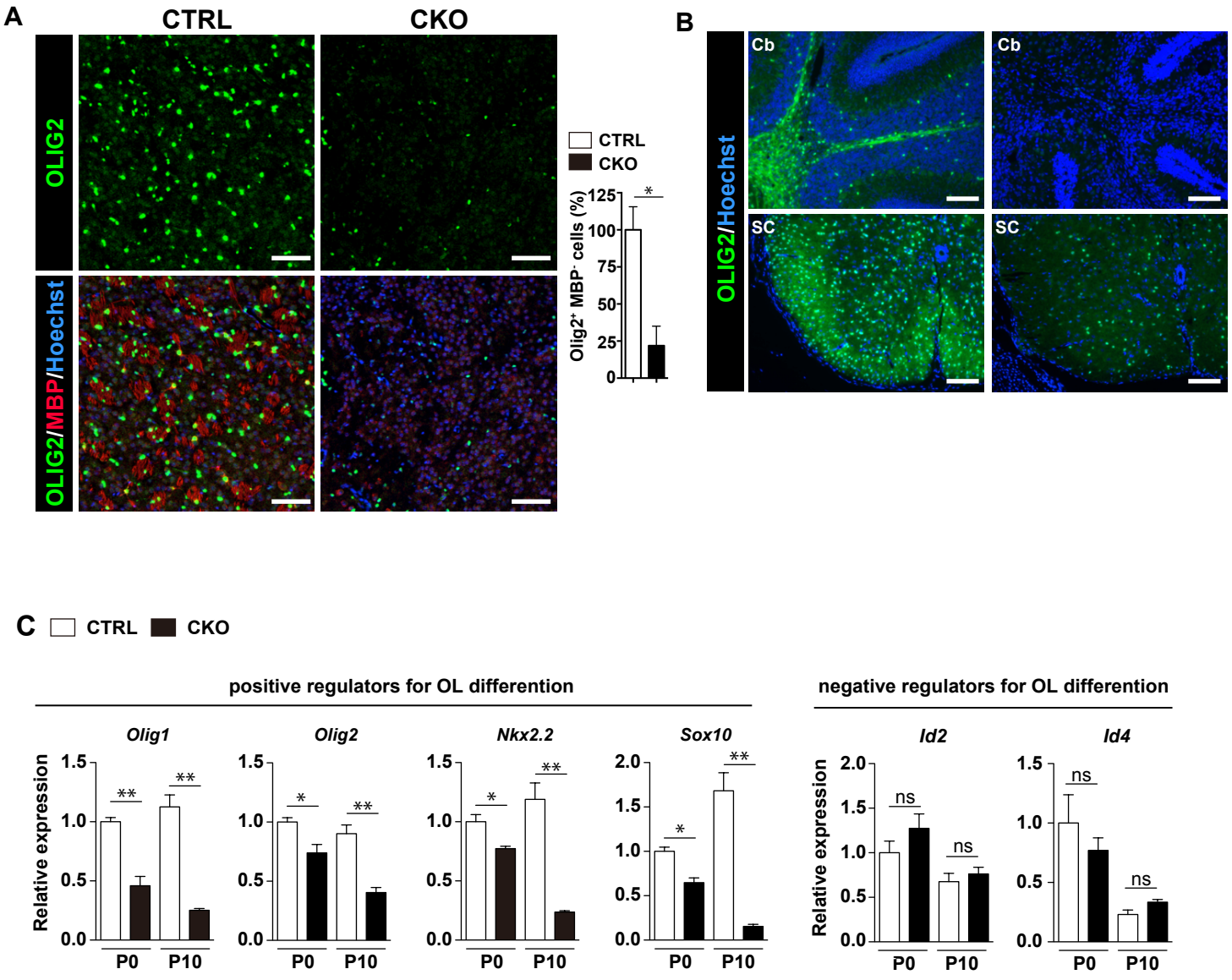

Fig. II-6. Oligodendrocyte lineage cells were reduced in *Prmt1*$^{flox/flox}$*; Nes-Cre* mice

(A) Immunostaining of OLIG2 (green) and MBP (red) with nuclear counterstain Hoechst (blue) in the striatum (Str) of CTRL and CKO mice at P10. The right graph shows the quantification of number of OLIG2+MBP- cells in the striatum. Numbers represent the average of three sections per each genotype from a single experiment. The data shown are mean ± SEM and analyzed by a two-tailed Student's t test. n=3 per each genotype. *$P < 0.05$ (B) Immunostaining of OLIG2 (green) with nuclear counterstain Hoechst (blue) in the cerebellum (Cb) and the spinal cord (SC) of CTRL and CKO mice at P10. (C) Relative gene expression of Olig1, Olig2, Nkx2.2, Sox10, Id2, and Id4 in the brain of CTRL and CKO mice at P0 and P10 as determined by quantitative RT-PCR. Normalized to Gapdh. All data shown are mean ± SEM and analyzed by a two-tailed Student's t test. n=4 per each genotype.*$P < 0.05$, ** $P < 0.01$ Scale bars represent 100 μm.

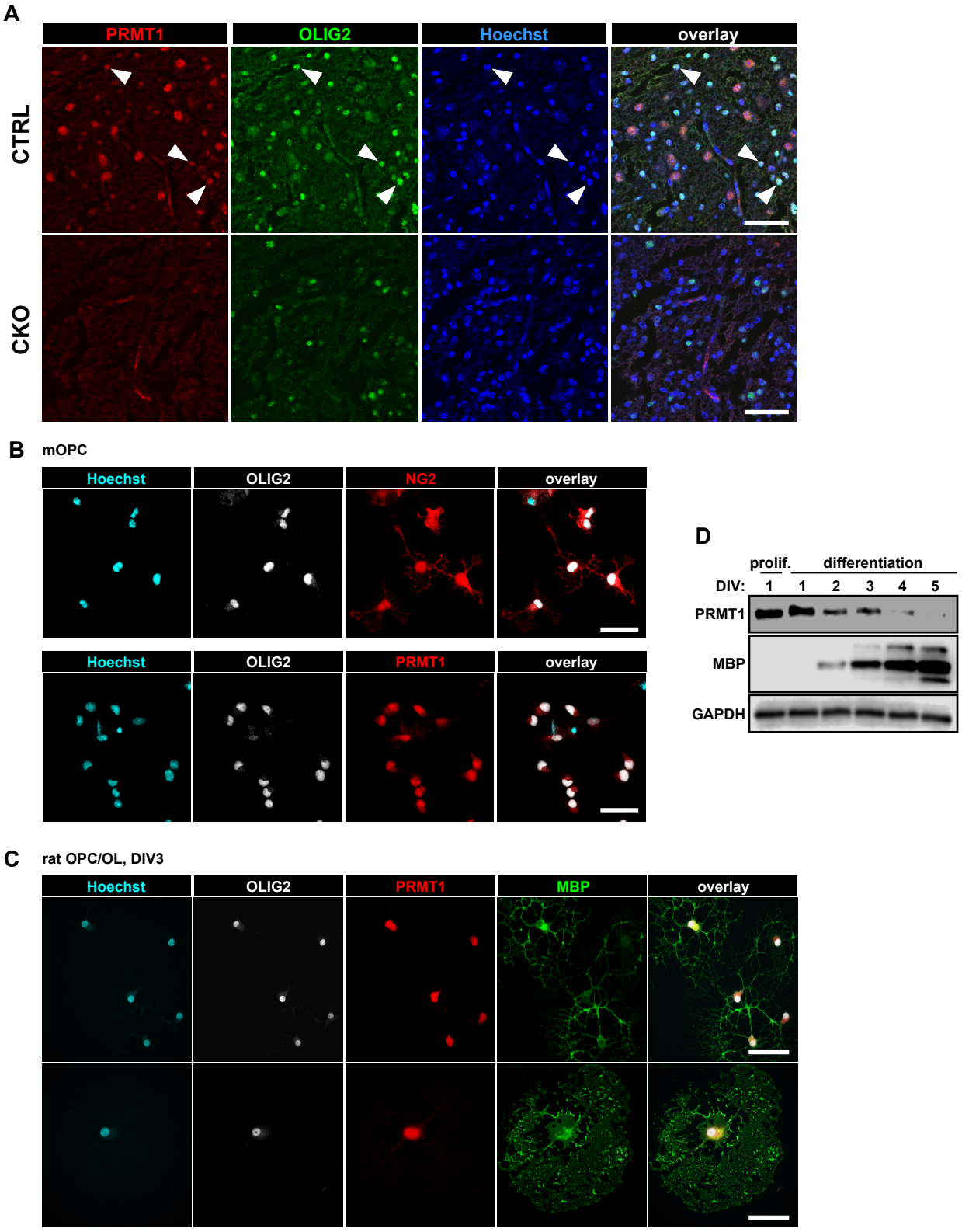

Fig. II-7. PRMT1 is expressed by oligodendrocyte lineage cells in vitro and in vivo

(A) Representative immunohistochemistry images in the cerebellar white matter of CTRL and CKO mice at P4. (B) Double-staining of OLIG2 with NG2 or PRMT1 on mouse OPCs cultured with growth factors. (C) Representative micrograph of co-labeling of OLIG2, MBP, and PRMT1 on differentiated rat oligodendrocytes at days in vitro (DIV) 3. (D) Western blot showing PRMT1 expression on primary rat cells at different stages of oligodendrocyte differentiation in vitro. MBP was used as a differentiation marker. prolif.: proliferation. DIV: days in vitro. Scale bars represent 50 μm in (A) and (C), and 30 μm in (B).

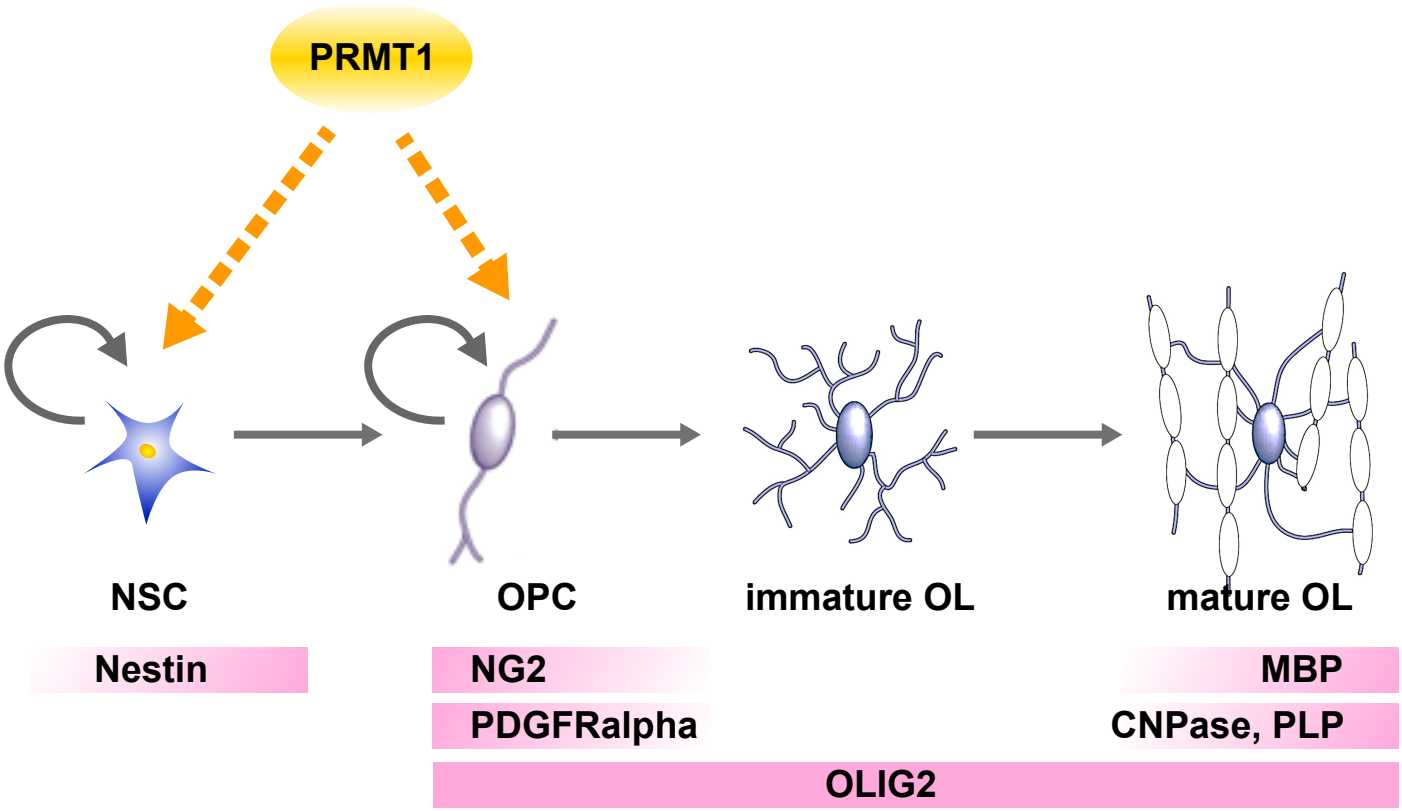

Fig. II-8. Speculated role of PRMT1 during CNS development

By loss of PRMT1 in NSCs, oligodendrocyte lineage development was suppressed in vivo. This result suggests a mechanistic model that PRMT1 positively regulates proliferation/differentiation potential of NSCs and/or OPCs directly or indirectly.

Table 1.

Genotypes of offspring obtained from the cross of *Prmt1*$^{flox/wt}$*; Nes-Cre* mice and *Prmt1*$^{flox/flox}$ mice.

Prmt1	*Cre*	Expected no. (%)	Observed no. (%)
fl/w	-	86 (25)	71 (21)
fl/w	+	86 (25)	90 (26)
fl/fl	-	86 (25)	109 (32)
fl/fl	+	86 (25)	73 (21)

The number (and percentage) of mice of various genotypes obtained by crosses of *Prmt1*$^{flox/wt}$*; Nes-Cre* and *Prmt1*$^{flox/flox}$ at P0 were shown. The expected number (and percentage) of mice was calculated according to the total number of mice born and based on the expected Mendelian 1:1:1:1 ratio.

Table 2.

The effect of overexpression of PRMT1 on the rate of oligodendrocyte differentiation.

		time after transfection		
cell markers	**vector transfected**	**24 h**	**48 h**	**56 h**
NG2	**Control**	65.22 ± 5.33	28.27 ± 8.26	16.22 ± 1.97
	Prmt1	51.40 ± 5.28	37.67 ± 6.06	17.24 ± 1.60
O4	**Control**	56.37 ± 12.90	57.88 ± 7.17	52.70 ± 11.36
	Prmt1	38.81 ± 7.23	59.49 ± 4.14	65.52 ± 9.27
MBP	**Control**	5.28 ± 2.24	28.53 ± 4.31	33.33 ± 3.45
	Prmt1	1.90 ± 2.23	32.84 ± 5.52	15.38 ± 5.72

The percentage of cells expressing differentiation markers including NG2, O4, or MBP were out of transfected cells which are confirmed by GFP expression. For each marker at each time point after transfection, results from control or Prmt1 transfected cells were compared and there were statistically no significant differences for all conditions by a two-tailed Student's *t* test. Percentages shown are the average of three 20x fields per coverslip from three to four coverslips per each condition. All data shown are mean ± SEM.

Chapter III.

Concluding Remarks

In the present study, I aimed to define the function of PRMT1 in the CNS development. For this objective, I generated CNS-specific PRMT1 knockout mice as a first genetic mutant with tissue-specific PRMT1 deletion. Unexpectedly, they prominently manifested oligodendrocyte lineage defect, resulting in severe dysmyelination at postnatal stages of development. However, they could survive postimplantation development although PRMT1 conventional knockout embryos have never survived (22). These results imply that PRMT1 is also required for early embryo in other tissues besides CNS. To elucidate why PRMT1 null embryo died, other models with conditional PRMT1 deletion will be needed by using other cell specific Cre-mediated gene recombination.

PRMT1-CKO mice were characterized by developmental CNS dysmyelination. Interestingly, OPCs survival, migration, proliferation, and differentiation/myelination occur during remyelination after demyelinating diseases such as multiple sclerosis (59-61). However, generally, the level of remyelination is insufficient and demyelinated lesions do not recover completely (59-61). As the present study focused on the role of PRMT1 in a developmental context, it would be interesting to know how PRMT1 activity influences NSCs and oligodendrocyte lineage cells during the recovery after demyelination. To investigate this, genetic ablation of PRMT1 using inducible Cre in NSCs or oligodendrocyte lineage cells would be a powerful tool.

In human, dysmyelination in newborn child is known in several diseases such as metachromatic leukodystrophy (MLD) and periventricular white matter injuries (PWMIs) (62, 63). PWMIs comprise periventricular leukomalacia (PVL) and diffuse white matter injury (DWMI) (63). Patients with these diseases are suffered from developing motor dysfunction and die at young age in many cases. In part of these syndromes, gene mutations are identified as a pathogenic mechanism, but not for all. The increasing number of PVL infants are born alive due to advancement of medicine, however, there is still no effective treatment for these patients (64). Previous papers have suggested that OPCs are the best target because their vulnerability to oxygen environment and cell death is evident in the white matter of these patients (65, 66). To understand the underlying mechanisms of failure in myelination in these patients, it is necessary to understand more about the precise regulations that control OPCs survival, proliferation, and differentiation.

Our CNS-specific PRMT1 knockout mice exhibited dysmyelination rather that demyelination, reminiscent of human dysmyelinating diseases. In the future, identification of responsible PRMT1 targets in NSCs and OPCs would surely help to give an answer how it regulates oligodendrocyte cell development and our mutant mice might serve as a genetic model to study the possible treatment of these syndromes.

Acknowledgments

I would like to express my deep gratitude to all those who provided me guidance, support and encouragement during the preparation of this dissertation. Most of all, I would like to express my sincere thanks to Professor Akiyoshi Fukamizu for all his support and guidance throughout my research work. I am deeply indebted to Dr. Junji Ishida, Dr. Juri Hamada, Dr. Kazuya Murata, Akihiko Kanou, Tomohiro Ishimaru, Professor Anna Williams, and Dr. Yoshitoshi Kasuya for excellent technical supports, invaluable guidance, and constructive discussions. I am also indebted to Yuko Jinzenji for technical support of electron microscopy. Finally, I appreciate greatly the helps of my parents and friends.

References

1. Bird, C.M., and Burgess, N. (2008) The hippocampus and memory: insights from spatial processing. *Nat.Rev.Neurosci.* **9,** 182-194

2. Tye, K.M., and Deisseroth, K. (2012) Optogenetic investigation of neural circuits underlying brain disease in animal models. *Nat.Rev.Neurosci.* **13,** 251-266

3. Araque, A., and Navarrete, M. (2010) Glial cells in neuronal network function. *Philos.Trans.R.Soc.Lond.B.Biol.Sci.* **365,** 2375-2381

4. Abbott, N.J., Ronnback, L., and Hansson, E. (2006) Astrocyte-endothelial interactions at the blood-brain barrier. *Nat.Rev.Neurosci.* **7,** 41-53

5. Sofroniew, M.V. (2015) Astrocyte barriers to neurotoxic inflammation. *Nat.Rev.Neurosci.* **16,** 249-263

6. Clarke, L.E., and Barres, B.A. (2013) Emerging roles of astrocytes in neural circuit development. *Nat.Rev.Neurosci.* **14,** 311-321

7. Nave, K.A. (2010) Myelination and the trophic support of long axons. *Nat.Rev.Neurosci.* **11,** 275-283

8. Sherman, D.L., and Brophy, P.J. (2005) Mechanisms of axon ensheathment and myelin growth. *Nat.Rev.Neurosci.* **6,** 683-690

9. Wake, H., Lee, P.R., and Fields, R.D. (2011) Control of local protein synthesis and initial events in myelination by action potentials. *Science.* **333,** 1647-1651

10. Martino, G., Pluchino, S., Bonfanti, L., and Schwartz, M. (2011) Brain regeneration in physiology and pathology: the immune signature driving therapeutic plasticity of neural stem cells. *Physiol.Rev.* **91,** 1281-1304

11. Li, X., and Jin, P. (2010) Roles of small regulatory RNAs in determining neuronal identity. *Nat.Rev.Neurosci.* **11,** 329-338

12. Hirabayashi, Y., and Gotoh, Y. (2010) Epigenetic control of neural precursor cell fate during development. *Nat.Rev.Neurosci.* **11,** 377-388

13. Bedford, M.T., and Clarke, S.G. (2009) Protein arginine methylation in mammals: who, what, and why. *Mol.Cell.* **33,** 1-13

14. Wolf, S.S. (2009) The protein arginine methyltransferase family: an update about function, new perspectives and the physiological role in humans. *Cell Mol.Life Sci.* **66,** 2109-2121

15. Tang, J., Frankel, A., Cook, R.J., Kim, S., Paik, W.K., Williams, K.R., Clarke, S., and Herschman, H.R. (2000) PRMT1 is the predominant type I protein arginine methyltransferase in mammalian cells. *J.Biol.Chem.* **275,** 7723-7730

1633. Huang, S., Litt, M., and Felsenfeld, G. (2005) Methylation of histone H4 by arginine methyltransferase PRMT1 is essential in vivo for many subsequent histone modifications. *Genes Dev.* **19,** 1885-1893

17. Wang, H., Huang, Z. Q., Xia, L., Feng, Q., Erdjument-Bromage, H., Strahl, B. D., Briggs, S. D., Allis, C. D., Wong, J., Tempst, P., and Zhang, Y. (2001) Methylation of histone H4 at arginine 3 facilitating transcriptional activation by nuclear hormone receptor. *Science* **293,** 853-857

18. Yamagata, K., Daitoku, H., Takahashi, Y., Namiki, K., Hisatake, K., Kako, K., Mukai, H., Kasuya, Y., and Fukamizu, A. (2008) Arginine methylation of FOXO transcription factors inhibits their phosphorylation by Akt. *Mol. Cell* **32,** 221-231

19. Zheng, S., Moehlenbrink, J., Lu, Y., Zalmas, L., Sagum, C. A., Carr, S., McGouran, J. F., Alexander, L., Fedorov, O., and Munro, S. (2013) Arginine methylation-dependent reader-writer interplay governs growth control by E2F-1. *Mol. Cell* **52,** 37-51

20. Teyssier, C., Ma, H., Emter, R., Kralli, A., and Stallcup, M. R. (2005) Activation of nuclear receptor coactivator PGC-1alpha by arginine methylation. *Genes Dev.* **19,** 1466-1473

21. Bulau, P., Zakrzewicz, D., Kitowska, K., Leiper, J., Gunther, A., Grimminger, F., and Eickelberg, O. (2007) Analysis of methylarginine metabolism in the cardiovascular system identifies the lung as a major source of ADMA. *Am. J. Physiol. Lung Cell. Mol. Physiol.* **292,** L18-24

22. Pawlak, M. R., Scherer, C. A., Chen, J., Roshon, M. J., and Ruley, H. E. (2000) Arginine N-methyltransferase 1 is required for early postimplantation mouse development, but cells deficient in the enzyme are viable. *Mol. Cell. Biol.* **20,** 4859-4869

23. Lin, W. J., Gary, J. D., Yang, M. C., Clarke, S., and Herschman, H. R. (1996) The mammalian immediate-early TIS21 protein and the leukemia-associated BTG1 protein interact with a protein-arginine N-methyltransferase. *J. Biol. Chem.* **271,** 15034-15044

24. Hong, E., Lim, Y., Lee, E., Oh, M., and Kwon, D. (2012) Tissue-specific and age-dependent expression of protein arginine methyltransferases (PRMTs) in male rat tissues. *Biogerontology* **13,** 329-336

25. Emery, B. (2010) Regulation of oligodendrocyte differentiation and myelination. *Science* **330,** 779-782

26. Ross, S. E., Greenberg, M. E., and Stiles, C. D. (2003) Basic helix-loop-helix factors in cortical development. *Neuron* **39,** 13-25

27. Rowitch, D. H. (2004) Glial specification in the vertebrate neural tube. *Nat. Rev. Neurosci.* **5,** 409-419

28. Copray, S., Huynh, J. L., Sher, F., Casaccia-Bonnefil, P., and Boddeke, E. (2009) Epigenetic mechanisms facilitating oligodendrocyte development, maturation, and aging. *Glia* **57,** 1579-1587

29. Dasgupta, B., and Milbrandt, J. (2009) AMP-activated protein kinase phosphorylates retinoblastoma protein to control mammalian brain development. *Dev. Cell* **16,** 256-270

30. Rafalski, V. A., Ho, P. P., Brett, J. O., Ucar, D., Dugas, J. C., Pollina, E. A., Chow, L. M., Ibrahim, A., Baker, S. J., and Barres, B. A. (2013) Expansion of oligodendrocyte progenitor cells following SIRT1 inactivation in the adult brain. *Nat. Cell Biol.* **15,** 614-624

31. Huang, J., Vogel, G., Yu, Z., Almazan, G., and Richard, S. (2011) Type II arginine methyltransferase PRMT5 regulates gene expression of inhibitors of differentiation/DNA binding Id2 and Id4 during glial cell differentiation. *J. Biol. Chem.* **286,** 44424-44432

32. Bezzi, M., Teo, S. X., Muller, J., Mok, W. C., Sahu, S. K., Vardy, L. A., Bonday, Z. Q., and Guccione, E. (2013) Regulation of constitutive and alternative splicing by PRMT5 reveals a role for Mdm4 pre-mRNA in sensing defects in the spliceosomal machinery. *Genes Dev.* **27,** 1903-1916

33. Chittka, A., Nitarska, J., Grazini, U., and Richardson, W. D. (2012) Transcription factor positive regulatory domain 4 (PRDM4) recruits protein arginine methyltransferase 5 (PRMT5) to mediate histone arginine methylation and control neural stem cell proliferation and differentiation. *J. Biol. Chem.* **287,** 42995-43006

34. Hamada, J., Baasanjav, A., Ono, N., Murata, K., Kako, K., Ishida, J., and Fukamizu, A. (2015) Possible involvement of downregulation of the apelin-APJ system in doxorubicin-induced cardiotoxicity. *Am. J. Physiol. Heart Circ. Physiol.* **308,** H931-41

35. Jarjour, A.A., Boyd, A., Dow, L.E., Holloway, R.K., Goebbels, S., Humbert, P.O., Williams, A., and ffrench-Constant, C. (2015) The polarity protein Scribble regulates myelination and remyelination in the central nervous system. *PLoS Biol.* **13,** e1002107

36. Bechler, M.E., Byrne, L., and Ffrench-Constant, C. (2015) CNS Myelin Sheath Lengths Are an Intrinsic Property of Oligodendrocytes. *Curr.Biol.* **25,** 2411-2416

37. Emery, B., and Dugas, J.C. (2013) Purification of oligodendrocyte lineage cells from mouse cortices by immunopanning. *Cold Spring Harb Protoc.* **2013,** 854-868

38. Tronche, F., Kellendonk, C., Kretz, O., Gass, P., Anlag, K., Orban, P. C., Bock, R., Klein, R., and Schutz, G. (1999) Disruption of the glucocorticoid receptor gene in the nervous system results in reduced anxiety. *Nat. Genet.* **23,** 99-103

39. Dhar, S., Vemulapalli, V., Patananan, A. N., Huang, G. L., Di Lorenzo, A., Richard, S., Comb, M. J., Guo, A., Clarke, S. G., and Bedford, M. T. (2013) Loss of the major Type I arginine methyltransferase PRMT1 causes substrate scavenging by other PRMTs. *Sci. Rep.* **3:** 1311

40. Readhead, C., Popko, B., Takahashi, N., Shine, H. D., Saavedra, R. A., Sidman, R. L., and Hood, L. (1987) Expression of a myelin basic protein gene in transgenic shiverer mice: correction of the dysmyelinating phenotype. *Cell* **48,** 703-712

41. Sidman, R. L., Dickie, M. M., and Appel, S. H. (1964) Mutant Mice (Quaking and Jimpy) with Deficient Myelination in the Central Nervous System. *Science* **144,** 309-311

42. Larocque, D., Pilotte, J., Chen, T., Cloutier, F., Massie, B., Pedraza, L., Couture, R., Lasko, P., Almazan, G., and Richard, S. (2002) Nuclear retention of MBP mRNAs in the quaking viable mice. *Neuron* **36,** 815-829

43. He, Y., Dupree, J., Wang, J., Sandoval, J., Li, J., Liu, H., Shi, Y., Nave, K. A., and Casaccia-Bonnefil, P. (2007) The transcription factor Yin Yang 1 is essential for oligodendrocyte progenitor differentiation. *Neuron* **55,** 217-230

44. Nave, K. (2010) Myelination and the trophic support of long axons. *Nat. Rev. Neurosci.* **11,** 275-283

45. Jahn, O., Tenzer, S., and Werner, H. B. (2009) Myelin proteomics: molecular anatomy of an insulating sheath. *Mol. Neurobiol.* **40,** 55-72

46. Lu, Q. R., Sun, T., Zhu, Z., Ma, N., Garcia, M., Stiles, C. D., and Rowitch, D. H. (2002) Common developmental requirement for Olig function indicates a motor neuron/oligodendrocyte connection. *Cell* **109,** 75-86

47. Takebayashi, H., Nabeshima, Y., Yoshida, S., Chisaka, O., Ikenaka, K., and Nabeshima, Y. (2002) The basic helix-loop-helix factor olig2 is essential for the development of motoneuron and oligodendrocyte lineages. *Curr. Biol.* **12,** 1157-1163

48. Qi, Y., Cai, J., Wu, Y., Wu, R., Lee, J., Fu, H., Rao, M., Sussel, L., Rubenstein, J., and Qiu, M. (2001) Control of oligodendrocyte differentiation by the Nkx2.2 homeodomain transcription factor. *Development* **128,** 2723-2733

49. Stolt, C.C., Rehberg, S., Ader, M., Lommes, P., Riethmacher, D., Schachner, M., Bartsch, U., and Wegner, M. (2002) Terminal differentiation of myelin-forming oligodendrocytes

depends on the transcription factor Sox10. *Genes Dev.* **16,** 165-170

50. Zhang, S.C. (2001) Defining glial cells during CNS development. *Nat.Rev.Neurosci.* **2,** 840-843

51. Zhang, Y., Chen, K., Sloan, S.A., Bennett, M.L., Scholze, A.R., O'Keeffe, S., Phatnani, H.P., Guarnieri, P., Caneda, C., Ruderisch, N., Deng, S., Liddelow, S.A., Zhang, C., Daneman, R., Maniatis, T., Barres, B.A., and Wu, J.Q. (2014) An RNA-sequencing transcriptome and splicing database of glia, neurons, and vascular cells of the cerebral cortex. *J.Neurosci.* **34,** 11929-11947

52. Nishiyama, A., Komitova, M., Suzuki, R., and Zhu, X. (2009) Polydendrocytes (NG2 cells): multifunctional cells with lineage plasticity. *Nat. Rev. Neurosci.* **10,** 9-22

53. Liu, Z., Hu, X., Cai, J., Liu, B., Peng, X., Wegner, M., and Qiu, M. (2007) Induction of oligodendrocyte differentiation by Olig2 and Sox10: evidence for reciprocal interactions and dosage-dependent mechanisms. *Dev. Biol.* **302,** 683-693

54. Kuspert, M., Hammer, A., Bosl, M. R., and Wegner, M. (2011) Olig2 regulates Sox10 expression in oligodendrocyte precursors through an evolutionary conserved distal enhancer. *Nucleic Acids Res.* **39,** 1280-1293

55. Zhou, Q., Choi, G., and Anderson, D. J. (2001) The bHLH transcription factor Olig2 promotes oligodendrocyte differentiation in collaboration with Nkx2.2. *Neuron* **31,** 791-807

56. Zhao, Q., Rank, G., Tan, Y. T., Li, H., Moritz, R. L., Simpson, R. J., Cerruti, L., Curtis, D. J., Patel, D. J., Allis, C. D., Cunningham, J. M., and Jane, S. M. (2009) PRMT5-mediated methylation of histone H4R3 recruits DNMT3A, coupling histone and DNA methylation in gene silencing. *Nat. Struct. Mol. Biol.* **16,** 304-311

57. Britsch, S., Goerich, D. E., Riethmacher, D., Peirano, R. I., Rossner, M., Nave, K. A., Birchmeier, C., and Wegner, M. (2001) The transcription factor Sox10 is a key regulator of peripheral glial development. *Genes Dev.* **15,** 66-78

58. Kim, H.J., Jeong, M.H., Kim, K.R., Jung, C.Y., Lee, S.Y., Kim, H., Koh, J., Vuong, T.A., Jung, S., Yang, H., Park, S.K., Choi, D., Kim, S.H., Kang, K., Sohn, J.W., Park, J.M., Jeon, D., Koo, S.H., Ho, W.K., Kang, J.S., Kim, S.T., and Cho, H. (2016) Protein arginine methylation facilitates KCNQ channel-PIP2 interaction leading to seizure suppression. *Elife.* **5,** 10.7554/eLife.17159

59. Franklin, R.J., and Ffrench-Constant, C. (2008) Remyelination in the CNS: from biology to therapy. *Nat.Rev.Neurosci.* **9,** 839-855

60. Pluchino, S., and Martino, G. (2008) The therapeutic plasticity of neural stem/precursor cells in multiple sclerosis. *J.Neurol.Sci.* **265,** 105-110

61. Huang, J.K., Jarjour, A.A., Nait Oumesmar, B., Kerninon, C., Williams, A., Krezel, W., Kagechika, H., Bauer, J., Zhao, C., Baron-Van Evercooren, A., Chambon, P., Ffrench-Constant, C., and Franklin, R.J. (2011) Retinoid X receptor gamma signaling accelerates CNS remyelination. *Nat.Neurosci.* **14,** 45-53

62. Kohlschutter, A., and Eichler, F. (2011) Childhood leukodystrophies: a clinical perspective. *Expert Rev.Neurother.* **11,** 1485-1496

63. Gallo, V., and Deneen, B. (2014) Glial development: the crossroads of regeneration and repair in the CNS. *Neuron.* **83,** 283-308

64. Back, S.A., Riddle, A., and McClure, M.M. (2007) Maturation-dependent vulnerability of perinatal white matter in premature birth. *Stroke.* **38,** 724-730

65. Volpe, J.J. (2001) Neurobiology of periventricular leukomalacia in the premature infant. *Pediatr.Res.* **50,** 553-562

66. Zonouzi, M., Scafidi, J., Li, P., McEllin, B., Edwards, J., Dupree, J.L., Harvey, L., Sun, D., Hubner, C.A., Cull-Candy, S.G., Farrant, M., and Gallo, V. (2015) GABAergic regulation of cerebellar NG2 cell development is altered in perinatal white matter injury. *Nat.Neurosci.* **18,** 674-682